

Reversible Migratory Insertion/ β -Alkyl Elimination in α -Agostic Alkylniobium Alkyne Complexes

Michel Etienne,* René Mathieu, and Bruno Donnadiu

Contribution from the Laboratoire de Chimie de Coordination du CNRS, UPR 8241, 205 Route de Narbonne, 31077 Toulouse Cedex 4, France

Received October 23, 1996[⊗]

Abstract: Ethyl-, *n*-propyl- and [(trimethylsilyl)methyl]niobium (4e)-alkyne complexes $\text{Tp}^*\text{Nb}(\text{Cl})(\text{CH}_2\text{R})(\text{PhC}\equiv\text{CR}')$ (Tp^* = hydrotris(3,5-dimethylpyrazolyl)borate; R = Me, R' = Me (**2a**), Et (**2b**), *n*-Pr (**2c**); R = Et, R' = Me (**3a**), Et (**3b**); R = SiMe₃, R' = Me (**4a**)) exhibit α -agostic structures in solution (¹H and ¹³C NMR) and in the solid state (X-ray structure at 173 K for **4a**). The phenylpropyne complexes **2a**, **3a**, and **4a** undergo a thermally induced rearrangement which yields niobium methyl complexes $\text{Tp}^*\text{Nb}(\text{Cl})(\text{Me})(\text{PhC}\equiv\text{CEt})$, $\text{Tp}^*\text{Nb}(\text{Cl})(\text{Me})(\text{PhC}\equiv\text{C}-n\text{-Pr})$, and $\text{Tp}^*\text{Nb}(\text{Cl})(\text{Me})(\text{PhC}\equiv\text{CCH}_2\text{SiMe}_3)$, respectively. This reaction follows a first-order rate law. The rate decreases with increased steric bulk of the alkyl group in the starting complex. For **2a**, a full kinetic analysis yields a high enthalpic barrier and an entropy of activation close to zero. Heating a toluene solution of $\text{Tp}^*\text{Nb}(\text{Cl})(n\text{-Pr})(\text{PhC}\equiv\text{CEt})$ (**3b**) establishes a 1:1 equilibrium between **3b** itself and $\text{Tp}^*\text{Nb}(\text{Cl})(\text{Et})(\text{PhC}\equiv\text{C}-n\text{-Pr})$ (**2c**). Heating a solution of $\text{Tp}^*\text{Nb}(\text{Cl})(\text{Et})(\text{PhC}\equiv\text{CEt})$ (**2b**) and $\text{PhC}\equiv\text{CMe}$ yields the η^1 -alkenyl (4e)-phenylpropyne complex $\text{Tp}^*\text{Nb}(\text{Cl})(\eta^1\text{-CPh}=\text{CEt}_2)(\text{PhC}\equiv\text{CMe})$ (**6**), demonstrating that alkyl migration is a key step of the rearrangement. Under pseudo-first-order conditions, this reaction does not depend on the phenylpropyne concentration. Potential 2e-donor ligands fail to act as efficient traps. Accordingly, a successful trapping experiment involves dinitrogen extrusion from $\text{N}_3\text{P}(\text{N}-i\text{-Pr}_2)_2$ in the presence of **2b** which yields an unprecedented (phosphinoimido)niobium complex: $\text{Tp}^*\text{Nb}(\text{Cl})(\eta^1\text{-CPh}=\text{CEt}_2)[=\text{N}-\text{P}(\text{N}-i\text{-Pr}_2)_2]$ (**7**). The crystal structure of **7** confirms the η^1 -alkenyl formulation and reveals a formal Nb–N triple bond, a linear Nb–N–P link, and a pyramidal P. Deoxygenation of propene oxide and desulfurization of ethylene sulfide gives, respectively, the oxo and sulfido η^1 -alkenyl complexes $\text{Tp}^*\text{Nb}(\text{Cl})(\eta^1\text{-CPh}=\text{CEt}_2)(=\text{X})$ (X = O (**8**), S (**9**)). The observed thermal rearrangements are unique examples of reversible migratory insertion/ β -alkyl elimination in transition metal alkyl alkyne complexes. In the absence of efficient trapping agent, the unsaturated η^2 -alkenyl intermediate that is first generated reversibly ring opens and ring closes. This realizes the intramolecular C–C bond activation which leads to the observed alkyl switch. Kinetic and trapping data indicate that the migratory insertion of the alkyl group on to the alkyne is the rate-determining step of the whole process.

Introduction

Although there are numerous reports of alkyne insertions into transition metal–hydrogen bonds, direct detection of migratory insertion of simple alkyl alkyne complexes and detailed studies of the reaction are rare.¹ Such studies are nonetheless highly desirable since this insertion represents a key step of the polymerization of alkynes via a vinyl pathway. In contrast to the wealth of work gathered with alkenes in connection with Ziegler–Natta catalysis,² little is known on alkyne insertion into early transition metal–alkyl bonds. Neutral scandocene³ and cationic titanocene,⁴ and zirconocene⁵ d⁰ alkyls, known to

catalyze ethylene polymerization, readily insert 1, and only 1 equiv of alkyne to give η^1 -vinyl species. Here the intermediate alkyl alkyne complexes are not detected. When the alkyl alkyne complexes are observed, they are reluctant to undergo the sought migratory insertion. This is typically the case of d² group 5 metal complexes. A subtlety could arise from the fact that the alkyne may behave as a flexible electron donor,⁶ but two striking examples that summarize the data suggest that this is not the case. Neither the 18-electron niobocene complexes of the type $\text{Cp}_2\text{Nb}(\text{R})(\text{alkyne})$ (Cp = $\eta^5\text{-C}_5\text{H}_5$, R = alkyl) which contain (2e)-alkyne ligands⁷ nor the formally unsaturated 16-electron complexes $\text{Cp}'\text{NbMe}_2(\text{alkyne})$ ⁸ or $\text{Cp}'\text{Nb}(\text{Me})(\text{Cl})(\text{alkyne})$ ⁹ (Cp' = $\eta^5\text{-C}_5\text{H}_4\text{Me}$) containing (4e)-alkyne ligands show any propensity to undergo the migratory insertion of the niobium alkyl on to the alkyne.

The microscopic reverse of the migratory insertion, namely, β -alkyl elimination, is now recognized as a major chain transfer step in Ziegler–Natta catalysis with d⁰ metal complexes.¹⁰ This decomposition of a metal–alkyl complex is an intramolecular activation of a $\text{Csp}^3\text{–Csp}^3$ bond, *a priori* a high-energy

* Corresponding author; e-mail: etienne@lcc-toulouse.fr.

[⊗] Abstract published in *Advance ACS Abstracts*, March 15, 1997.

(1) (a) Collman, J. P.; Hegedus, L. S.; Norton, J. R.; Finke, R. G. *Principles and Applications of Organotransition Metal Chemistry*; University Science Books: Mill Valley, 1987. (b) Otsuka, S.; Nakamura, A. *Adv. Organomet. Chem.* **1976**, *14*, 245. (c) *Comprehensive Organometallic Chemistry*; Abel, E. W., Stone, F. G. A., Wilkinson, G., Eds.; Pergamon: Oxford, U.K., 1982; Vol. 8. (d) *Comprehensive Organometallic Chemistry II*; Hegedus, L. S., Abel, E. W., Stone, F. G. A., Wilkinson, G., Eds.; Pergamon: Oxford, U.K., 1995; Vol. 12. (e) Huggins, J. H.; Bergman, R. G. *J. Am. Chem. Soc.* **1981**, *103*, 3002.

(2) (a) Fink, G., Müllhaupt, R., Brintzinger, H.-H., Eds. *Ziegler Catalysts*; Springer-Verlag: Berlin, 1995. (b) Brintzinger, H.-H.; Fischer, D.; Müllhaupt, R.; Rieger, B.; Waymouth, R. M. *Angew. Chem., Int. Ed. Engl.* **1995**, *34*, 1143. (c) Jordan, R. F. *Adv. Organomet. Chem.* **1991**, *32*, 325. (d) Bochman, M. J. *Chem. Soc., Dalton Trans.* **1996**, 255.

(3) Cotter, W. D.; Bercau, J. E. *J. Organomet. Chem.* **1991**, *417*, C1.

(4) Eisch, J. J.; Piotrowski, A. M.; Brownstein, S. K.; Gabe, E. J.; Lee, F. L. *J. Am. Chem. Soc.* **1985**, *107*, 7219.

(5) Jordan, R. F.; Lapointe, R. E.; Bradley, P. K.; Baezinger, N. *Organometallics* **1989**, *8*, 2892.

(6) Templeton, J. L. *Adv. Organomet. Chem.* **1989**, *29*, 1.

(7) Yasuda, H.; Yamamoto, H.; Arai, T.; Nakamura, A.; Chen, J.; Kai, Y.; Kasai, N. *Organometallics* **1991**, *10*, 4058.

(8) Curtis, M. D.; Real, J.; Hirpo, W.; Buthler, W. M. *Organometallics* **1990**, *9*, 66.

(9) Hirpo, W.; Curtis, M. D. *Organometallics* **1994**, *13*, 2706.

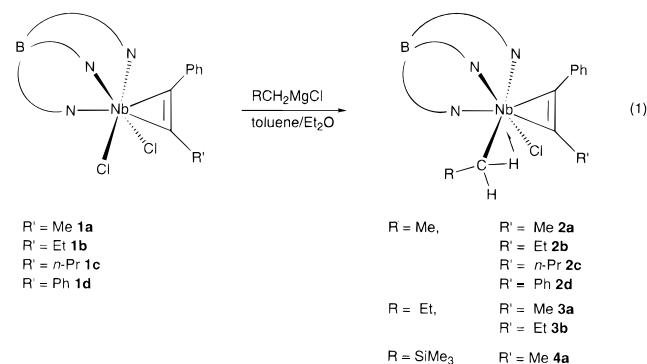
demanding process. To the best of our knowledge, such a reaction is unknown for alkenyl ligands, whether η^1 - or η^2 -coordinated.

In this paper, we report that 16-electron d^2 niobium α -agostic alkyl (4e)-alkyne complexes of the type $\text{Tp}^*\text{Nb}(\text{CH}_2\text{R})(\text{Cl})$ - (alkyne) ($\text{Tp}^* = \text{hydrotris}(3,5\text{-dimethylpyrazolyl})\text{borate}$, $\text{R} \neq \text{H}$), isolectronic with the Cp' complexes quoted above, undergo reversible migratory alkyne insertion/ β -alkyl elimination reactions in a single system. Synthetic work, including the successful trapping of alkenyl intermediates, as well as kinetic data and comparative studies lead to a reasonable description of the mechanism of the reaction. Solution (NMR) and solid state (X-ray diffraction) data suggest that an α -agostic interaction¹¹ might assist these fundamentally important reactions. Whether or not α -agostic interactions, either in the ground state or in the transition state, drive or assist alkene (or alkyne³) insertion in metallocene polymerization catalysis is still a topical question.¹² A preliminary account of this work has appeared.¹³

Results

Syntheses and Characterization of Alkyl Complexes.

Ethyl-, *n*-propyl-, and [(trimethylsilyl)methyl]niobium alkyne complexes $\text{Tp}^*\text{Nb}(\text{Cl})(\text{CH}_2\text{R})(\text{PhC}\equiv\text{CR}')$ ($\text{R} = \text{Me}$, $\text{R}' = \text{Me}$ (**2a**), Et (**2b**), *n*-Pr (**2c**); $\text{R} = \text{Et}$, $\text{R}' = \text{Me}$ (**3a**), Et (**3b**); $\text{R} = \text{SiMe}_3$, $\text{R}' = \text{Me}$ (**4a**)) are obtained in yields exceeding 80% from the reaction of 1 equiv of the appropriate chloro Grignard reagent with the dichloroniobium precursor¹⁴ $\text{Tp}^*\text{NbCl}_2(\text{PhC}\equiv\text{CR}')$ (eq 1). These complexes are isolated as room



temperature stable orange crystalline solids after recrystallization from toluene/alkane mixtures. Ethyl complexes $\text{Tp}^*\text{Nb}(\text{Cl})$ - ($\text{Et})(\text{R}'\text{C}\equiv\text{CR}')$ ($\text{R}' = \text{Ph}$ (**2d**), Me (**2e**)) containing symmetrical alkynes have also been obtained following the same procedure.

In addition to satisfactory elemental analyses, all of these complexes have been characterized by ^1H and ^{13}C NMR spectroscopies and in two cases, one of which is detailed below, by X-ray diffraction. Overall NMR features are as follows. Firstly, the niobium-bound alkyne carbons give low-field ^{13}C NMR resonances ($\delta > 215$) indicating the alkyne behaves as a 4e-donor. Thus, in addition to the formal Nb^{III} (d^2) formulation for these 16-electron species, a resonance form with the alkyne formally oxidizing the metal by two units, i.e., a Nb^{V} (d^0)

(10) (a) Hajela, S.; Bercaw, J. E. *Organometallics* **1994**, *13*, 1147. (b) Sini, G.; Macgregor, S. A.; Eisenstein, O.; Teuben, J. H. *Organometallics* **1994**, *13*, 1049. (c) Resconi, L.; Piemontesi, F.; Franciscono, G.; Abis, L.; Fiorani, T. *J. Am. Chem. Soc.* **1992**, *114*, 1025. (d) Yang, X.; Jia, L.; Marks, T. J. *J. Am. Chem. Soc.* **1993**, *115*, 3392. (e) Watson, P. L.; Parshall, G. W. *Acc. Chem. Res.* **1985**, *18*, 521. (f) Horton, A. D. *Organometallics* **1996**, *15*, 2675.

(11) Brookhart, M.; Green, M. L. H.; Wong, L.-L. *Prog. Inorg. Chem.* **1988**, *36*, 1.

(12) Grubbs, R. H.; Coates, G. W. *Acc. Chem. Res.* **1996**, *29*, 85.

(13) Etienne, M.; Biasotto, F.; Mathieu, R. *J. Chem. Soc., Chem. Commun.* **1994**, 1661.

(14) Etienne, M.; Biasotto, F.; Mathieu, R.; Templeton, J. L. *Organometallics* **1996**, *15*, 1106.

metallacyclopropene formulation, is an important contribution to the description of the bonding.⁶ We have adopted this formulation in the drawings. Secondly, complexes **2a–4a** are chiral and as such exhibit one resonance for each type of Tp^* hydrogen or carbon. Thirdly, complexes containing unsymmetrical phenylalkynes show the presence of two slowly interconverting rotamers at room temperature. They depend on the alkyne orientation with respect to Tp^* , and as detailed elsewhere,¹⁴ the rotamer with the phenyl group proximal to Tp^* is the more abundant. Only this isomer is shown in the drawings. Unless stated otherwise, all conclusions are valid for both isomers even if they are discussed for the major rotamer only. For the less bulky 2-butyne complex **2e**, the barrier to 2-butyne rotation has been measured ($\Delta G^\ddagger = 70 \text{ kJ mol}^{-1}$) from the coalescence of the Me signals at 360 K (^1H NMR, 250 MHz, toluene- d_8). The same barrier height is observed for the dichloro complex $\text{Tp}^*\text{NbCl}_2(\text{MeC}\equiv\text{CMe})$.¹⁴

Importantly, we can assign static α -agostic structures to these complexes on the basis of the following temperature independent (213–323 K) spectral features. In the ^1H NMR spectra, the diastereotopic α -methylene protons $\text{Nb}-\text{CH}_2\text{R}$ exhibit a very large chemical shift anisotropy. One proton is shielded around *ca.* δ 0.4 and the other one deshielded around *ca.* δ 3.8. They are coupled with $^2J_{\text{HH}}$ around 12–13 Hz. Additional coupling to the three protons of a methyl group is observed for the ethyl complexes **2a–e** ($\text{R} = \text{Me}$). These methyl groups appear as doublets of doublets with a smaller $^3J_{\text{HH}}$ with the shielded proton (*ca.* 6 Hz) than with the deshielded proton (*ca.* 7.5 Hz). In the case of *n*-propyl derivatives **3a,b**, the coupling patterns are complicated because of the presence of two other diastereotopic methylene protons on the β -carbon which appear at *ca.* δ 1.5 and 0.7. For the (trimethylsilyl)methyl derivative **4a**, there is no additional coupling so that the α -methylene protons appear as doublets ($^2J_{\text{HH}} = 12.2 \text{ Hz}$) centered at δ 3.40 and 0.34. The large chemical shift difference ($3.1 < \Delta\delta < 3.6$) is noteworthy for all the α -methylene protons.

In the ^{13}C NMR spectra, the niobium-bound carbons resonate as a broadened (10–30 Hz) doublet of doublets in the deshielded region δ 86–96 for the ethyl and *n*-propyl complexes. There is one reduced (103–108 Hz) and one enlarged (128–130 Hz) $^1J_{\text{CH}}$. In order to obtain more accurate values and assign the $^1J_{\text{CH}}$ to the proper hydrogen, $^1J_{\text{CH}}$ were measured from the ^{13}C satellites of the main ^1H NMR resonance (^1H NMR, 400 MHz) in the favorable cases where only one isomer is present. We have found accurate values of 105 and 128 Hz for, respectively, the shielded and deshielded proton resonances of the 2-butyne ethyl complex **2e**. For the diphenylethyne ethyl complex **2d** these values are, again respectively, 104 and 130 Hz. The smaller coupling constant is in both cases observed for the shielded proton. Similar data are obtained for the major isomer of the (trimethylsilyl)methyl phenylpropyne complex **4a** with $^1J_{\text{CH}} = 100 \text{ Hz}$ for the shielded proton.

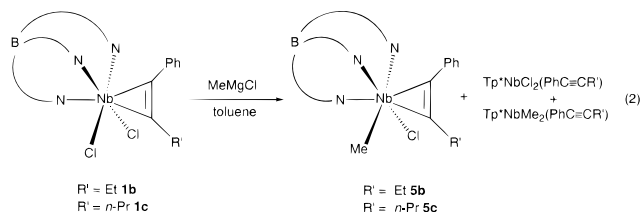
All of these data, including the fact that the shielded methylene proton is associated with the reduced $^1J_{\text{CH}}$, are definitive evidence of the presence of an α -agostic interaction between this hydrogen and the niobium.¹¹ They are fully reminiscent of those observed for α -agostic neopentylimidoniobium complexes.¹⁵ It is to be emphasized here that α -agostic interactions are rare when β -hydrogens are available.¹¹ The main reason for the preference of an α -agostic interaction in complexes **2–4** rests on the steric properties of Tp^* . Tp^* has a large cone angle (236°),¹⁶ and this precludes the sterically demanding bending of the alkyl group that would lead to a

(15) Poole, A. D.; Williams, D. N.; Kenwright, A. M.; Gibson, V. C.; Clegg, W.; Hockless, C. R.; O'Neil, P. A. *Organometallics* **1993**, *12*, 2549.

(16) Rheingold, A. L.; Ostrander, R. L.; Haggerty, B. S.; Trofimenko, S. *Inorg. Chem.* **1994**, *33*, 3666.

β -agostic interaction. Steric congestion around the metal in $[\text{Cp}^*\text{Hf}(\text{CH}_2\text{CHMe}_2)(\text{PMe}_3)]^+$ ($\text{Cp}^* = \eta^5\text{-C}_5\text{Me}_5$) also results in a preferred α -agostic interaction.¹⁷

Attempts to synthesize pure methyl chloro complexes $\text{Tp}^*\text{Nb}(\text{Cl})(\text{Me})(\text{PhC}\equiv\text{CR})$ ($\text{R} = \text{Et}$ (**5b**), $n\text{-Pr}$ (**5c**)) have been less successful. Treatment of the appropriate dichloro complex with 1 equiv of methyl lithium in toluene, even at -80°C , leads to a 1:1 mixture of dichloro and dimethyl¹⁴ derivatives. This behavior has been observed in related Cp derivatives. Dropwise addition of a THF solution of methylmagnesium chloride to a toluene solution of $\text{Tp}^*\text{NbCl}_2(\text{PhC}\equiv\text{CR})$ at -80°C gives a mixture containing ca. 80% of the desired $\text{Tp}^*\text{Nb}(\text{Cl})(\text{Me})(\text{PhC}\equiv\text{CR})$ contaminated by ca. 10% of each of the dichloro and dimethyl complexes. When THF is removed from the Grignard solution before mixing with the toluene solution of the dichloro complex, the purity of the chloro methyl complexes can be improved to ca. >90% (eq 2). Dimethylzinc is too mild



a reagent to methylate $\text{Tp}^*\text{NbCl}_2(\text{PhC}\equiv\text{CEt})$. The addition of a catalytic amount of AlCl_3 to a mixture of isopropyl chloride and $\text{Tp}^*\text{NbMe}_2(\text{PhC}\equiv\text{CEt})$, as described previously for the synthesis of $\text{Cp}^*\text{Ta}(\text{Cl})(\text{Me})(\text{ArC}\equiv\text{CAr})$ from the dimethyl derivative,⁹ leads to extensive decomposition, particularly of Tp^* itself.

Inequivalence of each set of protons and carbons of Tp^* in the ^1H and ^{13}C NMR spectra of **5b,c** confirms the lack of symmetry plane. For **5b**, the niobium-bound methyl gives a ^1H NMR singlet at δ 1.58 and, in the ^{13}C NMR spectrum, a niobium-broadened quartet centered at δ 64.6 with $^1J_{\text{CH}} = 122$ Hz. The diastereotopic propargylic methylene protons are identified in the ^1H NMR spectrum by an AB quartet (δ 4.08 and 3.90, $^2J_{\text{HH}} = 11$ Hz) and in the ^{13}C NMR spectrum by a triplet ($^1J_{\text{CH}} = 122$ Hz) at δ 31.6. Similar data have been obtained in the Cp^* series.⁹

Probing the presence of agostic interactions in methyl complexes is extremely difficult.¹¹ At least, this requires the synthesis of D-isotopomers and the systematic study of their dynamic behavior by ^1H NMR.^{11,18} Even in favorable cases where dynamic isotope effects have been probed,^{19,20} the topic is still under debate.²¹ Thus we are reluctant to propose a definitive structure on a sound basis here, although some debatable factors might suggest the absence of significant agostic interactions in **5b,c**.²²

X-ray Molecular Structure of the (Trimethylsilyl)methyl Complex 4a. The α -agostic interaction observed in solution is also present in the solid state. We have previously obtained an X-ray crystal structure of the ethyl complex **2b**.²³ However the data were quite poor, and the α -hydrogens were not located. A shortened Nb–C α bond of 2.17(2) Å and an opened Nb–C α –C β angle of 126(1) $^\circ$ suggested that an α -agostic interaction

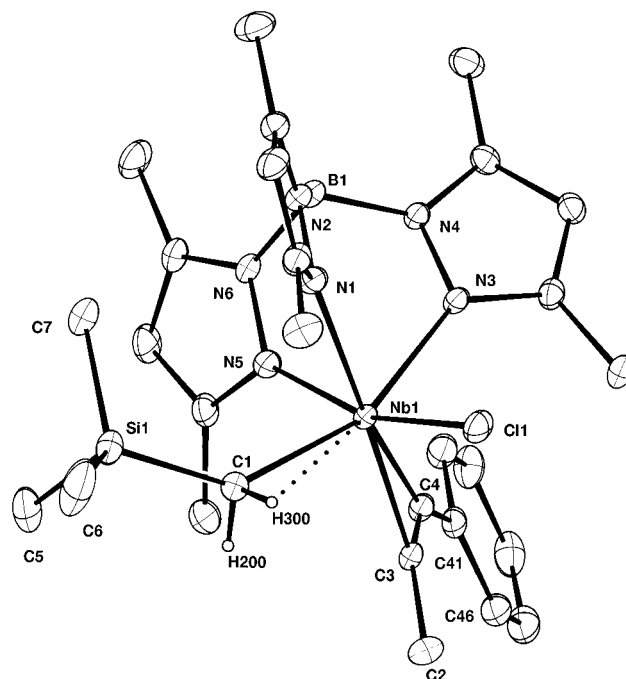


Figure 1. Plot of the molecular structure of $\text{Tp}^*\text{Nb}(\text{Cl})(\text{CH}_2\text{SiMe}_3)(\text{PhC}\equiv\text{CMe})$ (**4a**). Located and refined H are shown.

was indeed present.²³ Since then we have obtained good quality crystals of the (trimethylsilyl)methyl complex **4a** that have been analyzed by X-ray diffraction at 173 K. A summary of crystal data can be found in Table 1, and Table 2 presents important bond lengths and angles. A perspective view of the complex is shown in Figure 1. We do not discuss the overall structure which is fully comparable to those of other compounds of the type $\text{Tp}^*\text{Nb}(\text{X})(\text{Y})(\text{alkyne})$. Short niobium–alkyne carbon bond lengths particularly characterize the (4e)-alkyne formulation and hence the participation of a niobacyclopentene form to an accurate description of the bonding. Focusing on the (trimethylsilyl)methyl ligand, we find a Nb–C bond length appropriate for a shortened single bond (Nb(1)–C(1) = 2.204(4) Å), and an opened angle around the α -carbon (Nb(1)–C(1)–Si(1) = 135.5(2) $^\circ$). Several hydrogen atoms were observed in a difference Fourier map although only those bound to C(1) were considered and refined isotropically. Hydrogen H(300) is in close proximity to the niobium whereas H(200) is not (Nb(1)–H(300) = 2.29(6) Å, Nb(1)–C(1)–H(300) = 84(4) $^\circ$, Nb(1)–H(200) = 2.67(4) Å, Nb(1)–C(1)–H(200) = 113(3) $^\circ$). These data are fully reminiscent of those observed by Gibson and co-workers for a bis(neopentyl)imidoniobium(V) complex.¹⁵ The data also allow us to secure the α -agostic interaction in the solid state structure of **2b**.²³ Interestingly, agostic H(300) lies between Nb(1), C(1), and Cl(1), a region of space where, according to EHMO calculations,²² there is a lobe of the LUMO. The other lobe of the LUMO which lies in the C–Nb–N(pyrazole) wedge is much less accessible on steric grounds.

Thermal Rearrangement of α -Agostic Complexes: Reversible Migratory Insertion of Alkyl Alkyne Complexes. All of the alkyl alkyne complexes described above are stable

(17) Guo, Z.; Swenson, D. C.; Jordan, R. F. *Organometallics* **1994**, *13*, 1424.

(18) Calvert, R. B.; Shapley, J. P. *J. Am. Chem. Soc.* **1978**, *100*, 7726.
(19) Dawoodi, Z.; Green, M. L. H.; Mtetwa, V. S. B.; Prout, K.; Schultz, A. J.; Williams, J. M.; Koetzle, T. J. *Chem. Soc., Dalton Trans.* **1986**, 1629.

(20) Green, M. L. H.; Hugues, A. K.; Popham, N. A.; Stephens, A. H. H.; Wong, L.-L. *J. Chem. Soc., Dalton Trans.* **1992**, 3077.

(21) Maus, D. C.; Copié, V.; Sun, B.; Griffiths, J. M.; Griffin, R. G.; Luo, S.; Schrock, R. R.; Liu, A. H.; Seidel, S. W.; Davis, W. M.; Grohman, A. *J. Am. Chem. Soc.* **1996**, *118*, 5665.

(22) **5b,c** are formally neutral Nb^{III} d^2 octahedral complexes and thus are not highly electrophilic. According to EHMO calculations, the HOMO–LUMO gap is 1.9 eV in the model compound $\text{TpNbCl}_2(\text{HC}\equiv\text{CH})$. To a first approximation, this indicates electronic saturation despite the formal 16e-count. Thus we suggest that the higher alkyl complexes **2a–e**, **3b,c**, and **4a** are α -agostic mainly because of important steric repulsions between the alkyl groups and Tp^* . The methyl group would be small enough so that no steric pressure would force any α -agostic interaction. See: Etienne, M.; Donnadiou, B.; Mathieu, R.; Fernandez-Baeza, J.; Jalon, F.; Otero, O.; Rodrigo-Blanco, M. E. *Organometallics* **1996**, *15*, 4597.

(23) Etienne, M. *Organometallics* **1994**, *13*, 410.

Table 1. Crystal Data, Data Collection, and Refinement Parameters for Tp*Nb(Cl)(CH₂SiMe₃)(PhC≡CMe)·Et₂O (**4a**·Et₂O) and Tp*Nb(Cl)(CPh=CEt₂)[=N-P(N-*i*-Pr₂)] (**7**)

	compd	
	4a·Et ₂ O	7
Crystal Data		
chemical formula	C ₃₂ H ₅₁ BClN ₆ NbOSi	C ₃₉ H ₆₅ BClN ₉ NbP
formula weight	703.06	830.15
crystal system	triclinic	triclinic
space group	<i>P</i> 1̄	<i>P</i> 1̄
<i>a</i> (Å)	10.679(6)	12.774(3)
<i>b</i> (Å)	13.050(9)	13.263(2)
<i>c</i> (Å)	13.725(9)	15.259(3)
α (deg)	85.54(6)	78.55(1)
β (deg)	69.97(5)	81.85(2)
γ (deg)	81.30(5)	61.55(2)
<i>V</i> (Å ³)	1780(4)	2225(1)
<i>Z</i>	2	2
ρ (anal. calcd) (Mg·m ⁻³)	1.31	1.24
crystal size (mm)	0.40 × 0.47 × 0.50	0.3 × 0.4 × 0.4
μ (cm ⁻¹)	4.64	3.89
Data Collection		
radiation (graphite monochr)	Mo K α ($\lambda = 0.71073$ Å)	Mo K α ($\lambda = 0.71073$ Å)
data collection method	$\omega/2\theta$	$\omega/2\theta$
temperature (K)	173	293
no. of measured reflns	6624	5019
no. of independent reflns	6256 ($R_m = 2.1$)	5019
no. of observed reflns	4961 [$I > 4\sigma(I)$]	2962 [$I > 3\sigma(I)$]
2θ max (deg)	50	52
scan range θ (deg)	1.1 + 0.35tg θ	0.8 + 0.35tg θ
Refinement		
refinement on	<i>F</i>	<i>F</i>
R^a	0.0426	0.039
R_w^b	0.0481	0.041
l s parameters	396	384
max rms shift	0.41	0.49
abs corr (corr)	psi scans (0.71–1)	none
weighting scheme ^c	$w = w'[1 - (\Delta F/6\sigma(F_o))^2]^2$	$w = w'[1 - (\Delta F/6\sigma(F_o))^2]^2$
coeff Ar	3.81, -1.86, 1.96, -0.319, -0.696	4.31, -6.52, 3.53, -1.91
goodness of fit, S^d	1.125	1.69

^a $R = \sum(|F_o| - |F_c|)/\sum|F_o|$. ^b $R_w = [\sum w(|F_o| - |F_c|)^2/\sum w|F_o|^2]^{1/2}$. ^c $w' = 1/\sum(r = 1,3)\text{ArTr}(x)$, where Ar are the coefficients for the Chebyshev polynomial $\text{Tr}(x)$ with $x = F_o/F_c(\text{max})$. ^d Goodness of fit $S = [\sum(|F_o - F_c|)^2/(N_{\text{obs}} - N_{\text{parameters}})]^{1/2}$.

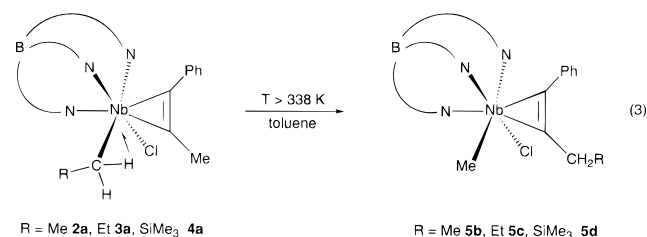
Table 2. Selected Bond Lengths (Å) and Angles (deg) for Tp*Nb(Cl)(CH₂SiMe₃)(PhC≡CMe)·Et₂O (**4a**·Et₂O)

Bond Lengths			
Nb(1)–Cl(1)	2.4247(8)	Nb(1)–N(1)	2.340(3)
Nb(1)–C(1)	2.204(4)	Nb(1)–N(3)	2.275(3)
Nb(1)–C(3)	2.065(3)	Nb(1)–N(5)	2.259(3)
Nb(1)–C(4)	2.078(3)	C(3)–C(4)	1.305(5)
Nb(1)–H(200)	2.67(4)	Si(1)–C(1)	1.869(4)
Nb(1)–H(300)	2.29(6)		
Bond Angles			
Nb(1)–C(1)–H(200)	113(3)	Nb(1)–C(1)–H(300)	84(4)
Nb(1)–C(1)–Si(1)	135.5(2)	Cl(1)–Nb(1)–C(1)	104.3(1)
Cl(1)–Nb(1)–N(1)	83.34(7)	Cl(1)–Nb(1)–N(3)	89.74(7)
Cl(1)–Nb(1)–N(5)	164.23(7)	Cl(1)–Nb(1)–N(5)	164.23(7)
N(1)–Nb(1)–N(3)	78.33(9)	N(1)–Nb(1)–N(5)	84.0(1)
N(3)–Nb(1)–N(5)	78.54(9)	N(1)–Nb(1)–C(1)	85.9(1)
N(3)–Nb(1)–C(1)	157.6(1)	N(5)–Nb(1)–C(1)	84.0(1)

at room temperature for days either in the solid state or as solutions in toluene. However, under thermal activation, some of them undergo a rearrangement which exchanges the niobium-bound alkyl group and the alkyne alkyl group. This rearrangement is based on the reversible migratory insertion of the alkyl group on to the alkyne. A transient unsaturated alkenyl species is generated which may either undergo intramolecular C–C bond activation leading to the alkyl switch or be trapped with appropriate reagents, as shown later.

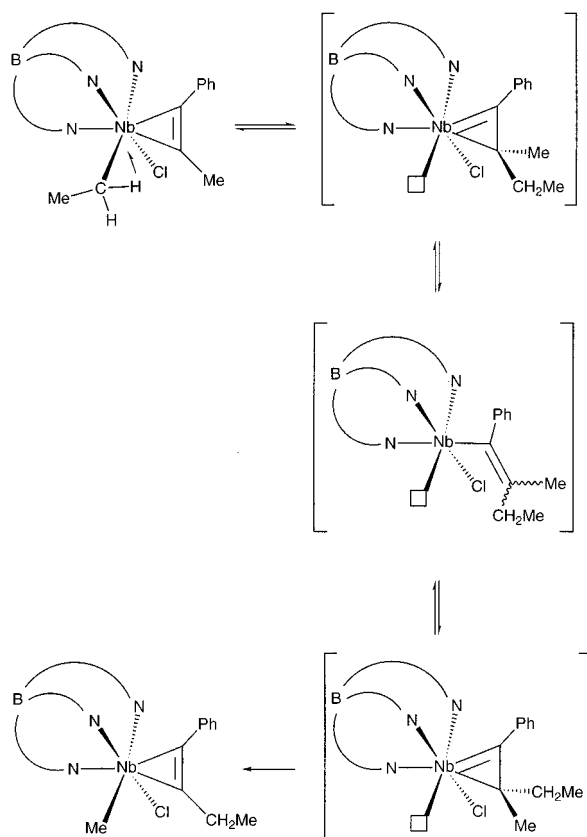
When heated above 338 K in toluene (either in a Schlenk tube on a half-millimole scale or in NMR tubes) the α -agostic ethyl, *n*-propyl, and (trimethylsilyl)methyl complexes **2a**, **3a**,

and **4a** containing *phenylpropyne* as the alkyne rearrange to niobium *methyl* complexes containing respectively phenylbutyne **5b**, phenylpentyne **5c**, and 1-phenyl-3-(trimethylsilyl)prop-1-yne **5d** as the alkyne (eq 3), as ascertained by ¹H and ¹³C NMR



(decoupled and gated decoupled). **5b,c** obtained in this way give spectroscopic data identical with those of **5b,c** obtained from **1b,c** and MeMgCl as described above. Furthermore, treatment of the material obtained after thermolysis of **2a** with 1 equiv of methyllithium yields quantitatively the known dimethyl derivative Tp*NbMe₂(PhC≡CEt).¹⁴ In the ¹H NMR spectrum of Tp*Nb(Cl)(Me)(PhC≡CCH₂SiMe₃) (**5d**), the propargylic methylene protons give an AB quartet (δ 4.09 and 3.91, each d, $J = 10.8$ Hz), and the niobium-bound methyl group appears at δ 1.56. In the ¹³C NMR spectrum, the propargylic carbon appears as a triplet ($J_{\text{CH}} = 122$ Hz) at δ 31.6, and the niobium-bound carbon gives a characteristic quartet ($J_{\text{CH}} \approx 122$ Hz) at δ 64.6. The methyl signals of the trimethylsilyl group in **5d** are deshielded (¹H NMR, δ 0.50), whereas they are shielded in agostic **4a** (δ -0.20).

Scheme 1



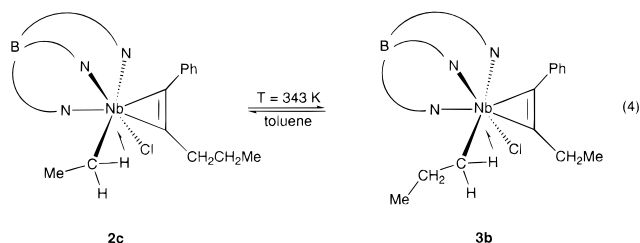
As judged from *in situ* NMR spectroscopy and isolated material, the methylniobium complex is formed in *ca.* 80% yield. Dichloro complexes containing the rearranged alkyne, but significantly no dichloro complexes of the unrearranged alkyne, are formed in *ca.* 10%. Some ill-defined products giving several NMR resonances account for less than *ca.* 10% of the yield. All of these reactions go to completion.

A likely mechanism, based on the formation of two types of unsaturated alkenyl species, is depicted in Scheme 1. We show later that this is indeed the best description of the reaction.

Additional relevant experimental data are as follows. In these systems containing phenylalkylalkynes, we have only observed cases of $\equiv\text{C}-\text{Csp}^3$ activation with no competition of the $\equiv\text{C}-\text{ipsoPh}$ activation reaction. Similarly there is no rearrangement in the diphenylethyne niobium ethyl complex **2d**. More surprisingly, the 2-butyne niobium ethyl complex **2e** is also reluctant to undergo this exchange reaction. The phenylpropyne benzyl complex²³ $\text{Tp}^*\text{Nb}(\text{Cl})(\text{CH}_2\text{Ph})(\text{PhC}\equiv\text{CMe})$ decomposes extensively to several ill-defined products upon heating above 343 K. Recall here that there is no evidence for α -agostic interactions in this complex.²³

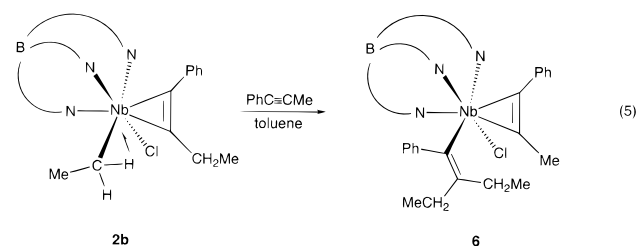
When the alkyl group on the alkyne is not methyl, the reaction is reversible. When the *phenylbutyne ethyl* complex **2c** is heated overnight at 343 K in toluene, clean equilibration ($K_{\text{eq}} \approx 1.0$) with the *phenylbutyne n-propyl* complex **3b** occurs as ascertained by ¹H NMR spectroscopy (eq 4). In a control experiment, **3b** is similarly converted to a 1:1 mixture of **3b** and **2c**. The thermal rearrangement of the ethyl phenylbutyne complex **2b** is degenerate; consequently no change is observed by ¹H NMR.

These experiments give conclusive evidence for an overall exchange between the niobium-bound alkyl groups and the alkyl group of the alkyne as suggested above by the experiments with the phenylpropyne complexes. However, with the higher alkyls, this exchange is reversible. It may be understood as a real metathesis between $\text{Nb}-\text{Csp}^3$ and coordinated $\text{Csp}-\text{Csp}^3$ bonds.



Trapping Experiments. All of our complexes exist as mixtures of rotamers, and in order to simplify the NMR interpretations for the trapping reactions, we have chosen the phenylbutyne ethyl complex **2b** since its rearrangement is degenerate.

First it must be emphasized that thermolysis of **2b** in the presence of potential 2e-donor ligands such as trimethylphosphine, pyridine, or ethylene does not lead to trapped products. Only **2b** can be observed by ¹H NMR. However, a clean reaction converts in 75% yield a mixture of **2b** and phenylpropyne to the analytically and spectroscopically characterized η^1 -alkenyl phenylpropyne complex $\text{Tp}^*\text{Nb}(\text{Cl})(\eta^1\text{-CPh}=\text{CET}_2)(\text{PhC}\equiv\text{CMe})$ (**6**) (eq 5). The reaction is regioselective, no



isomer with an ethyl group bound to the α -carbon being observed. The coordinated alkyne is indeed phenylpropyne *not* phenylbutyne. The X-ray structure of a related compound confirms the η^1 -alkenyl formulation (see below).

Prominent ¹³C NMR data indicate that phenylpropyne acts as a 4e-donor (δ 249.7 and 224.1, $\text{Nb}(\text{PhC}\equiv\text{CMe})$)⁶ and that the alkenyl is η^1 -bound to the metal (δ 204.9 (br, $\text{Nb}-\text{C}\alpha$) and 149.3 ($\text{C}\beta$)).²⁴ The two CH_2 's bound to $\text{C}\beta$ resonate at δ 26.5 and 24.0 ($^1J_{\text{CH}} = 125$ Hz with a quartet fine structure), and the methyl group of the alkyne gives a quartet ($^1J_{\text{CH}} = 129$ Hz) centered at δ 21.1. In the ¹H NMR spectrum, the phenyl group bound to $\text{C}\alpha$ gives five separate resonances. Two inequivalent ethyl groups, bound to $\text{C}\beta$, give similar patterns with close chemical shifts, as opposed to the situation found in **2a**. Although formal electron count, oxidation state, and orbital matching would be unchanged,⁶ the alternative coordination possibility of a (2e)-alkyne with an η^2 -(4e)-alkenyl is not adopted. This observation correlates with the lack of effective trapping with potential 2e-donor ligands.

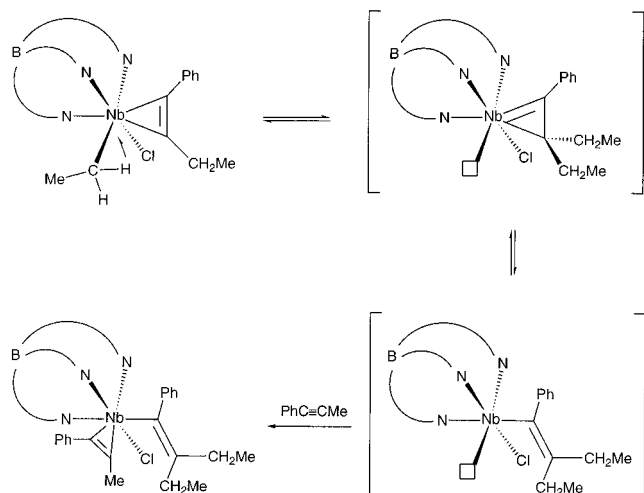
Thus the rearrangement, whether reversible or not (for the phenylpropyne complexes) occurs via migratory insertion of an alkyl group on to the alkyne and its microscopic reverse, β -alkyl elimination. These observations are summarized in Scheme 2. It is the first time that such fundamentally important events are directly observed in the case of alkynes. The reaction is known for olefins in d^0 systems, where both reactions are relevant to Ziegler–Natta processes.^{2,10} Direct observation of reversible migratory insertion/ β -methyl elimination at a ruthenium center has been observed recently.²⁵

The need for potentially 4e-donor ligands is further demonstrated by the thermal reaction of **2a** with a phosphino azide, propylene oxide, or ethylene sulfide. Such reactions should lead

(24) Herberich, G. E.; Mayer, H. *Organometallics* **1990**, *9*, 2655.

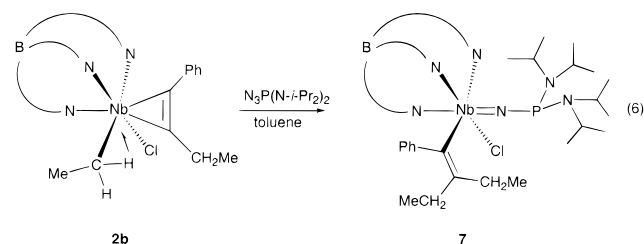
(25) McNeill, K.; Andersen, R. A.; Bergman, R. G. *J. Am. Chem. Soc.* **1995**, *117*, 3625.

Scheme 2



to imido-, oxo-, or sulfidoniobium(V) complexes, respectively, via either N₂ extrusion or O or S abstraction. As already mentioned, (4e)-alkyne ligands impart Nb^V (d⁰) character to the formally Nb^{III} (d²) complexes.⁶

The thermal reaction of **2a** with an organic azide follows a well-established route to imido metal complexes.²⁶ The phosphino azide N₃P(N-*i*-Pr)₂ cleanly reacts with **2b** to give in high yield the η^1 -alkenyl imidoniobium(V) complex Tp*⁺Nb(Cl)(η^1 -CPh=CEt₂)[=N-P(N-*i*-Pr)₂] (**7**) (eq 6). The η^1 -



alkenyl moiety is spectroscopically characterized as above. Diastereotopic isopropyl groups are observed in the ¹H and ¹H-³¹P{¹H} NMR spectra. In the ³¹P{¹H} NMR spectrum, a singlet at δ 118.7 characterizes a trivalent pyramidal phosphorus bound to three nitrogens.²⁷ Heteroatom-functionalized imido ligands are not common. Haloimido²⁸ and hydrazido²⁹ compounds are known, but few examples of thioalkoxyl (=N-SR)³⁰ and, very recently, alkoxyimido (=N-OR)³¹ complexes have been reported. Phosphorane iminato complexes (=N=PR₃) and phosphorus(V)-substituted imido complexes (=N-P(X)R₂, X = O, S) are also known, particularly for niobium itself.³² However the phosphinoimido complex (=N-PR₂) we describe here is unique, and an X-ray crystal structure of this complex has been obtained.

X-ray Crystal Structure of Tp*⁺Nb(Cl)(η^1 -CPh=CEt₂)[=N-P(N-*i*-Pr)₂] (7**).** A summary of crystallographic data

(26) Wigley, D. E. *Prog. Inorg. Chem.* **1994**, 42, 239.

(27) Leroux, Y.; Burgada, R.; Kleeman, S. G.; Fluck, E. In *CRC Handbook of Phosphorus-31 Nuclear Magnetic Resonance Data*; Tebb, J. C., Ed.; CRC Press: Boca Raton, FL, 1987; p 93.

(28) Dehnicke, K.; Strahle, J. *Chem. Rev.* **1993**, 93, 981.

(29) Sutton, D. *Chem. Rev.* **1993**, 93, 995.

(30) Bishop, M. W.; Chatt, J.; Dilworth, J. R.; Hursthouse, M. B.; Motevalle, M. J. *Less-Common Met.* **1977**, 54, 487.

(31) Green, M. L. H.; James, J. T.; Sanders, J. F. *Chem. Commun.* **1996**, 1343.

(32) (a) Dehnicke, K.; Strahle, J. *Polyhedron* **1989**, 8, 707. (b) Weller, F.; Nusszar, D.; Dehnicke, K. *Z. Anorg. Allg. Chem.* **1992**, 615, 7. (c) Olms, P.; Roesky, H. W.; Keller, K.; Noltemeyer, M. *Z. Naturforsch., Teil B* **1992**, 47, 1609. (d) Nusszar, D.; Weller, F.; Dehnicke, K.; Hiller, W. *J. Alloys Compd.* **1992**, 183, 30.

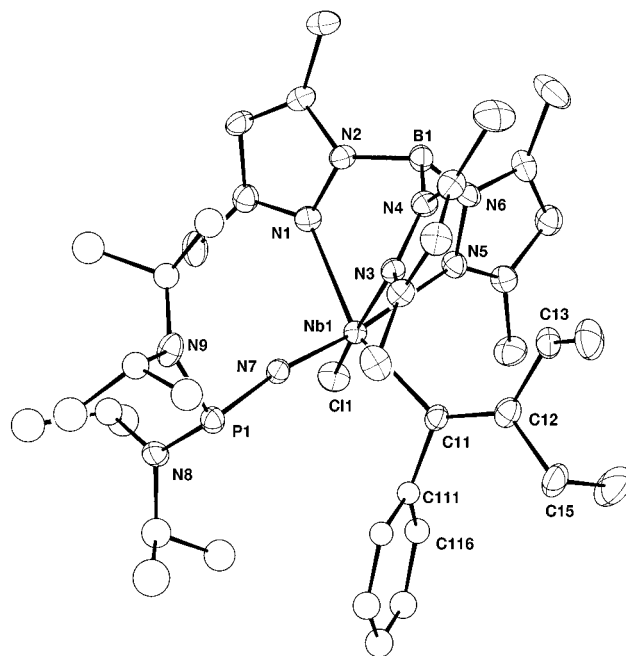


Figure 2. Plot of the molecular structure of Tp*⁺Nb(Cl)(CPh=CEt₂)(=N-P(N-*i*-Pr)₂) (**7**). Ellipsoids are drawn at the 30% probability level for clarity.

Table 3. Selected Bond Lengths (Å) and Angles (deg) for Tp*⁺Nb(Cl)(CPh=CEt₂)[=N-P(N-*i*-Pr)₂] (**7**)

Bond Lengths			
Nb(1)–Cl(1)	2.363(1)	Nb(1)–N(1)	2.307(6)
Nb(1)–C(11)	2.252(7)	Nb(1)–N(3)	2.271(4)
P(1)–N(7)	1.731(5)	Nb(1)–N(5)	2.450(4)
P(1)–N(8)	1.689(5)	Nb(1)–N(7)	1.779(4)
P(1)–N(9)	1.695(5)	C(11)–C(12)	1.354(8)
Bond Angles			
Cl(1)–Nb(1)–N(1)	94.4(1)	Cl(1)–Nb(1)–N(3)	166.2(1)
Cl(1)–Nb(1)–N(5)	84.9(1)	Cl(1)–Nb(1)–N(7)	97.7(1)
Cl(1)–Nb(1)–C(11)	96.6(1)	N(1)–Nb(1)–N(3)	79.3(2)
N(1)–Nb(1)–N(5)	75.2(2)	N(1)–Nb(1)–N(7)	98.2(2)
N(1)–Nb(1)–C(11)	158.7(2)	N(3)–Nb(1)–N(5)	81.6(1)
N(3)–Nb(1)–N(7)	95.4(2)	N(3)–Nb(1)–C(11)	85.8(2)
N(5)–Nb(1)–N(7)	173.1(2)	N(5)–Nb(1)–C(11)	87.7(2)
N(7)–P(1)–N(8)	106.7(3)	N(7)–P(1)–N(9)	99.4(2)
N(8)–P(1)–N(9)	108.1(3)	Nb(1)–N(7)–P(1)	170.8(4)
Nb(1)–C(11)–C(12)	131.7(5)	Nb(1)–C(11)–C(111)	112.5(4)
C(12)–C(11)–C(111)	115.3(6)	C(11)–C(12)–C(13)	125.6(7)
C(11)–C(12)–C(15)	121.4(6)	C(13)–C(12)–C(15)	113.0(6)

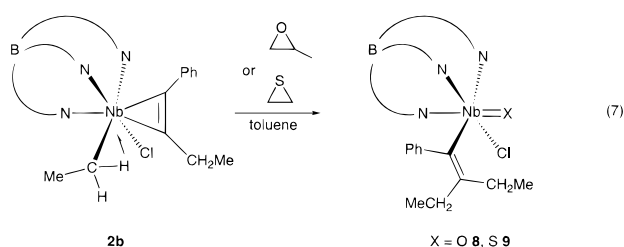
is presented in Table 1, and relevant bond distances and angles can be found in Table 3. A perspective view of the molecule is given in Figure 2. The overall geometry around Nb(1) is that of a distorted octahedron. The stereochemistry of the alkenyl ligand is confirmed: a phenyl group is attached to C α , and C β bears two ethyl groups. Examination of the angles around C(11) (bound to Nb(1)) and C(12) confirms the sp² hybridization of these carbons and the η^1 -alkenyl formulation. C(11)–C(12) is a typical C–C double bond (1.354(8) Å). The Nb(1)–C(11) bond length (2.252(7) Å) is appropriate for a single bond between Nb^V and Csp². In the Nb^{III} d², 18e- complex Cp₂Nb(Me₃SiC≡CSiMe₃)[η^1 -C(CO₂Me)=CH(CO₂Me)],²⁴ Nb–C α is 2.297(5) Å. The alkenyl ligand sits in a wedge formed by two *cis*-pyrazole rings with one ethyl group pointing toward these rings.

The bis(diisopropylamino)phosphinoimido ligand exerts a strong *trans* effect. The *trans*-niobium–N–pyrazole bond length is at least 0.15 Å longer than the other ones. The imido ligand is virtually linear around the imido nitrogen (Nb(1)–N(7)–P(1) = 170.8(4)°). This deviation from strict linearity is not uncommon in this type of complex.²⁶ The Nb(1)–N(7) bond

length of 1.779(4) Å lies slightly above the average value of *ca.* 1.76 Å for monoimido niobium(V) complexes,²⁶ but values up to 1.812(3) Å for CpNb(=NAr)(=CHPh)(PMe₃) have been recorded.³³ It is consistent with a formal Nb–N triple bond. This suggests the lone pair on the sp-hybridized nitrogen is involved in a pπ–dπ bonding with the metal.²⁶ The Nb–N bond length and Nb–N–P angle do not seem to be influenced by the presence of the phosphorus. Examination of the figure and of the angles around P(1) clearly indicates that the phosphorus remains pyramidal, *i.e.*, the lone pair of the sp³ phosphorus does not contribute with the imido lone pair to the bonding with the electron deficient niobium. Instead the Nb–N bond length remains normal (see above), and P(1)–N(7) is longer (*ca.* 0.04 Å at 1.731(5) Å) than the bonds between P(1) and the amino nitrogens N(8) and N(9). In the isoelectronic alkoxy-substituted imidoniobium complex CpNbCl₂(=N–O–*t*-Bu),³¹ the N–O bond similarly remains a single bond (N–O = 1.342(5) Å) and the oxygen is sp³-hybridized. One angle around P(1) is conspicuously less obtuse than the others (N(7)–P(1)–N(9) = 99.4(2) Å). The bis(diisopropylamino) group is thus directed toward Tp*, again in a wedge formed by two pyrazole rings. This distortion, although disfavored on steric grounds, directs the lone pair of P(1) away from N(7). This suggests that there may be some repulsion between the formal lone pairs of electrons on P(1) and N(7).

This X-ray structure definitely establishes the η¹-alkenyl formulation of the trapped products and indicates that, despite the steric bulk of Tp*, a crowded imido ligand can be coordinated to Nb. Since the phosphorus is still pyramidal, some chemistry at the available lone pair can be envisioned.

Reaction between **2b** and either propylene oxide or ethylene sulfide leads to oxygen or sulfur atom abstraction and again to formation of η¹-alkenyl niobium(V) complexes (eq 7). The oxo and sulfido complexes Tp*Nb(X)(Cl)(η¹-CPh=CEt₂) (X = O, **8**; S, **9**) are isolated in good yields as highly colored bright red (X = O) or dark red-purple (X = S) crystals. Their ¹H and ¹³C NMR spectra are entirely comparable to those of the other η¹-CPh=CEt₂ complexes. They exhibit virtually superimposable infrared spectra except for the Nb=X vibrations which are observed at 930 cm⁻¹ (X = O) and 514 cm⁻¹ (X = S).



These reactions further support the mechanism of alkyl exchange but also demonstrate that the unsaturated Nb^{III} d² intermediate is reactive. Such oxygen or sulfur atom abstraction utilizing group 5 metal^{III} complexes is known. Previously the unsaturated intermediates were generated by hydride to methylenide migration in Cp₂Ta(H)(CH₂)³⁴ or displacement of ethylene in Cp₂Ta(C₂H₄)(CH₃)³⁵. Isolable triamido amine vanadium(III) complexes behave similarly.³⁶ To our knowledge it is the first time that alkyl migration is used to effect this reaction.

(33) Cockcroft, J. K.; Gibson, V. C.; Howard, J. A. K.; Poole, A. D.; Stenling, U.; Wilson, C. *J. Chem. Soc., Chem. Commun.* **1992**, 1668.

(34) Whinnery, L. L.; Henling, L. M.; Bercaw, J. E. *J. Am. Chem. Soc.* **1991**, *113*, 7575.

(35) Proulx, G.; Bergman, R. G. *Organometallics* **1996**, *15*, 133.

(36) Cummins, C. C.; Schrock, R. R.; Davis, W. M. *Inorg. Chem.* **1994**, *73*, 1448.

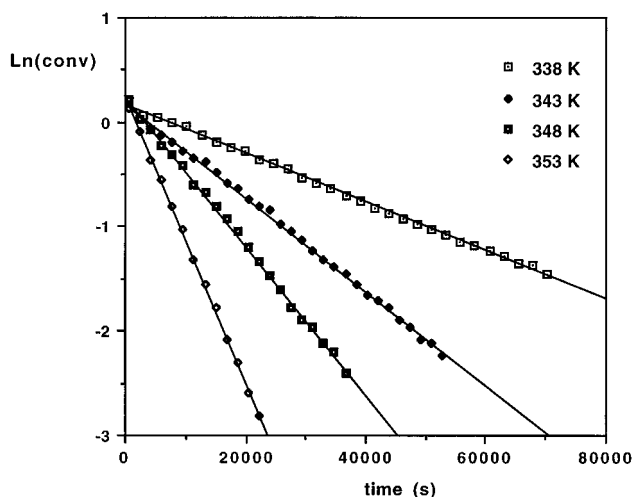


Figure 3. First-order kinetic plots for the rearrangement of **2a** (curve fit as straight lines with $r^2 = 0.999$). Corresponding k values can be found in Table 4.

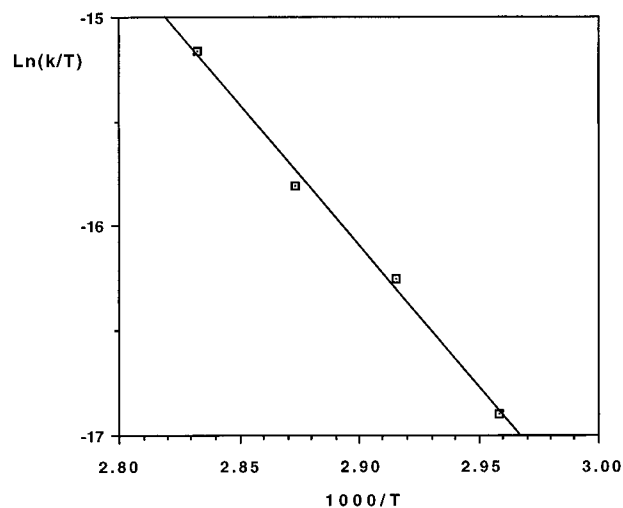


Figure 4. Eyring plot of the data of Table 4 (curve fit as a straight line with $r^2 = 0.995$).

Table 4. First-Order Kinetic Data for the Thermolysis of Tp*Nb(Cl)(CH₂Me)(PhC≡CMe) (**2a**)^a

temperature (K)	$k_{\text{obs}} 10^5$ (s ⁻¹)
338	1.55 ± 0.10
343	3.0 ± 0.1
348	4.8 ± 0.1
353	9.2 ± 0.1

^a Toluene-*d*₈, [**2a**] ≈ 4 × 10⁻² M, ¹H NMR 250 MHz.

Kinetic Data. We have obtained simple kinetic data on the rearrangement of phenylpropyne complexes **2a**, **3a**, and **4a**. Their thermolyses were followed *in situ* by ¹H NMR in toluene-*d*₈ at a reference temperature of 343 K. A more detailed analysis at four different temperatures has been carried out in the case of the ethyl complex **2a**. The experimental rate data are shown in Figure 3 and Table 4, and the associated Eyring plot is presented in Figure 4. The disappearance of all of the three complexes follows a first-order rate law. No intermediates are observed. The rate constants for the disappearance of **2a** and **3a** at 343 K are virtually equal within estimated experimental error $k_{343}(\mathbf{2a}) = (3.0 \pm 0.1) \times 10^{-5} \text{ s}^{-1}$ and $k_{343}(\mathbf{3a}) = (2.9 \pm 0.1) \times 10^{-5} \text{ s}^{-1}$. However, with the more bulky (trimethylsilyl)methyl group, the rate constant is smaller $k_{343}(\mathbf{4a}) = (2.3 \pm 0.1) \times 10^{-5} \text{ s}^{-1}$. These observations are consistent with the fact that relief of steric congestion (which is operative when going from the higher alkyl complexes to the methyl complexes)

Table 5. Pseudo-First-Order Kinetic Data for the Reaction of $\text{Tp}^*\text{Nb}(\text{Cl})(\text{CH}_2\text{Me})(\text{PhC}\equiv\text{CCH}_2\text{Me})$ (**2b**) with $\text{PhC}\equiv\text{CMe}^a$

run	PhC≡CMe/ 2b ratio	$k_{\text{obs}}10^5$ (s ⁻¹)
1	5.7	3.7
2	7.9	3.1
3	7.8	3.4
4	12.2	3.3

^a Toluene-*d*₈, [**2a**] $\approx 4 \times 10^{-2}$ M, ¹H NMR 250 MHz.

is not a driving force of the reaction. The 1:1 equilibrium observed for the rearrangement of the higher alkyls **2c** and **3b** may be correlated with the similar rate constants for the rearrangement of the phenylpropyne ethyl and *n*-propyl complexes **2a** and **3a**. The rearrangement of **2a** occurs with a quite high activation enthalpy ($\Delta H^\ddagger = 113 \pm 5$ kJ mol⁻¹) and a near zero activation entropy ($\Delta S^\ddagger = 4 \pm 12$ J K⁻¹ mol⁻¹). This is consistent with little reorganization in the transition state as compared to the starting complex.

At the reference temperature of 343 K, the reaction between the phenylbutyne ethyl complex **2b** and phenylpropyne leading to the alkenyl complex **6** follows a pseudo-first-order behavior when the alkyne:**2b** ratio varies between *ca.* 6 and 12 (Table 5). The magnitude of k_{obs} ($(3.4 \pm 0.3) \times 10^{-5}$ s⁻¹) is to be compared to the first-order rate constant k_{343} ($(3.0 \pm 0.1) \times 10^{-5}$ s⁻¹) for the rearrangement of **1a**. Their comparable magnitude shows that the trapping is efficient and that the migration of the alkyl group on to the alkyne is the rate-determining step of the rearrangement. This is also consistent with the high enthalpic barrier observed for the rearrangement of **1a**.

Discussion

The results reported above establish an unprecedented thermally induced reversible migratory insertion/ β -alkyl elimination in (4e)-alkyne α -agostic alkylniobium complexes. These reactions are of utmost interest since they represent key steps of fundamental organometallic chemistry that should have important consequences in our understanding of alkyne polymerization. We summarize here some of the key features that lead to a reasonable description of the mechanism of the reaction.

As suggested above, the migratory insertion of an alkyl group on a (4e)-alkyne should eventually lead to an η^2 -(4e)-alkenyl compound.⁶ Nucleophilic attack on a coordinated alkyne has been studied thoroughly in the case of (2e)-alkyne iron complexes³⁷ and in the case of (4e)-alkyne group 6 complexes.³⁸ This reaction yields, respectively, η^1 -(2e)-alkenyls or η^2 -(4e)-alkenyls. For the (4e)-alkyne complexes, there has been no evidence ever that the nucleophile attacks the metal first and then migrates on to the alkyne.³⁸ In this way, our results describe the first observation of a migratory insertion of an alkyl group on to a (4e)-alkyne. However the trapping experiments reveal η^1 -(2e)-alkenyl complexes with an additional 4e-ligand. The reason why an η^2 -(4e)-alkenyl is not isolated most likely resides on steric grounds. The niobium-bound β -carbon of an η^2 -(4e)-alkenyl is formally sp³-hybridized, and, with two alkyl groups, it is far too bulky in the crowded Tp^* environment. Thus, the first step of the rearrangement (Scheme 2) generates an unsaturated η^2 -(4e)-alkenyl intermediate which can either reversibly ring open (to give an η^1 -alkenyl) and ring close or react with an entering molecule. It is more likely that reaction with the trap occurs at the η^1 -alkenyl stage since the intermediate

should then be even more electrophilic. If no trapping occurs C–C bond activation *i.e.*, β -alkyl elimination, occurs, accounting for the observed reversibility.

As observed for migratory insertions of alkene hydride³⁹ and alkene alkyl⁴⁰ complexes, the activation entropy is close to 0. This suggests little reorganization on proceeding to the transition state. The high enthalpic barrier for the rearrangement of **2a** and the similar magnitude of the rate constants for the trapping of **2b** by phenylpropyne ($k_{\text{obs}} = (3.4 \pm 0.3) \times 10^{-5}$ s⁻¹) and for the rearrangement of **2a** ($k_{343} = (3.0 \pm 0.1) \times 10^{-5}$ s⁻¹) are noteworthy. These observations are consistent with a rate-determining migration of the alkyl group. Significantly, all of the complexes that rearrange exhibit an α -agostic interaction in the ground state. However, we have no evidence that the α -agostic interaction is required. In the absence of kinetic isotope effect studies, we are not able to probe more accurately the transition state. This mechanistic scheme is akin to the so-called modified Green–Rooney mechanism for alkene polymerization.¹¹ Such a mechanism would not be followed in d⁰ systems where α -agostic interactions would be involved in the transition state only.¹² We again point to the fact that the ground state α -agostic interaction mainly results from the steric properties of Tp^* . From the X-ray structure of **4a**, this α -agostic interaction does not lead to important geometrical distortions that would suggest an interaction between the α -carbon and the coordinated carbon of the alkyne, *i.e.*, an incipient C–C bond. However, the bulky trimethylsilyl group sits in a wedge formed by two pyrazole rings away from the alkyne so that the methylene group is set up for the migration. The rearrangement of the phenylpropyne complexes, which generates niobium methyl complexes, goes to completion. This is depicted for complex **2a** in Scheme 1. The lack of (observed) reversibility might be correlated to the fact that transition metal–methyl bonds are stronger by *ca.* 15 ± 5 kJ mol⁻¹ than other simple transition metal–alkyl bonds.⁴¹ This again addresses the question of the presence of significant α -agostic interaction in the methyl complexes.²²

The examination of migratory aptitudes of the alkyl groups gives further evidence for the importance of steric effects. The rearrangement of the phenylpropyne ethyl complex **2a** is faster ($k_{343} = 3.0 \times 10^{-5}$ s⁻¹) than that of the more bulky phenylpropyne (trimethylsilyl)methyl complex **4a** ($k_{343} = 2.3 \times 10^{-5}$ s⁻¹), even if relief of steric congestion is undoubtedly more important for **4a** than for **2a**.

Finally the β -alkyl elimination, as depicted in Schemes 1 and 2, is unlikely to occur at the η^1 -alkenyl stage for obvious geometrical reasons. In the absence of a trapping molecule no other reaction competes with this intramolecular C–C bond activation in the η^2 -alkenyl intermediate. Obviously there is an entropic reason for this, but this also results from the high thermodynamic preference for the octahedral chloro alkyl alkyne complexes. No C–H activation product resulting from α -hydrogen abstraction which would have been facilitated by the α -agostic interaction is observed. This is accounted for by the (4e)-alkyne description that imparts a high degree of d⁰, Nb^V character to the metal, as already mentioned.

Conclusion

The major advances reported in this article are the direct observation of a reversible migratory insertion/ β -alkyl elimina-

(37) (a) Reger, D. L.; Belmore, K. A.; Mintz, E.; McElligott, P. J. *Organometallics* **1984**, *3*, 134. (b) Reger, D. L. *Acc. Chem. Res.* **1988**, *21*, 229.

(38) Allen, S. R.; Beevor, R. G.; Green, M.; Norman, N. C.; Orpen, A. G.; Williams, I. D. *J. Chem. Soc., Dalton Trans.* **1985**, 435.

(39) (a) Burger, B. J.; Santarsiero, B. D.; Trimmer, M. S.; Bercaw, J. E. *J. Am. Chem. Soc.* **1988**, *110*, 3134. (b) Brookhart, M.; Hauptman, E.; Lincoln, D. M. *J. Am. Chem. Soc.* **1992**, *114*, 10394.

(40) (a) Rix, F.; Brookhart, M. *J. Am. Chem. Soc.* **1995**, *117*, 1137. (b) Rix, F. C.; Brookhart, M.; White, P. S. *J. Am. Chem. Soc.* **1996**, *118*, 4746.

(41) Dias, A. R.; Diogo, H. P.; Griller, D.; Minas de Piedade, M. E.; Martinho Simoes, J. A. In *Bonding Energetics in Organometallic Compounds*; ACS Symposium Series 428; Marks, T. J., Ed.; American Chemical Society: Washington, DC, 1990; pp 205–217.

tion in α -agostic alkyniobium alkyne complexes and a first attempt to describe the mechanism of these fundamentally important reactions by means of kinetic and trapping experiments. The rarely observed migratory insertion of an alkyne into a niobium-alkyl bond is the rate-determining step of the whole process. It is the first time that such a reaction and its microscopic reverse, β -alkyl elimination, are described for (4e)-alkyne complexes. Among the trapped products, a new functionalized phosphinoimido complex has been fully characterized.

Experimental Section

All reactions and workup procedures were performed under an atmosphere of dried dinitrogen using conventional vacuum line and Schlenk tube techniques. Toluene was dried and distilled by refluxing over sodium-benzophenone under argon. *n*-Hexane and pentane were dried and distilled over calcium hydride under dinitrogen. Methylmagnesium chloride (3.0 M in THF), ethylmagnesium chloride (2.0 M in diethyl ether), *n*-propylmagnesium chloride (2.0 M in diethyl ether), [(trimethylsilyl)methyl]magnesium chloride (1.0 M in diethyl ether), alkynes, propylene oxide, and ethylene sulfide were used as received from commercial sources. The following chemicals were prepared according to published procedures: $\text{Tp}^*\text{NbCl}_2(\text{PhC}\equiv\text{CR}')^{14}$ and $\text{N}_3\text{P}(\text{N}-i\text{-Pr})_2$. (Caution: hazardous material, potentially explosive!)⁴² Benzene-*d*₆ and toluene-*d*₈ were stored over molecular sieves under dinitrogen. NMR data were acquired on Bruker AC 200, AM 250, or, in some cases, AMX 400 spectrometers at room temperature in benzene-*d*₆ unless otherwise cited. IR data have been obtained in KBr pellets on a FT-IR Perkin-Elmer 1725 spectrophotometer. Elemental analyses were performed in the Analytical Service of our laboratory.

Synthesis of α -Agostic Alkyl Complexes 2a-e, 3a,b, and 4a. All of these complexes were synthesized following the same procedure described in detail for $\text{Tp}^*\text{Nb}(\text{Cl})(\text{Et})(\text{PhC}\equiv\text{CMe})$ (**2a**). To a vigorously stirred toluene (30 mL) solution of $\text{Tp}^*\text{NbCl}_2(\text{PhC}\equiv\text{CMe})$ (**1a**) (0.840 g, 1.45 mmol) cooled to -25°C was added dropwise under dinitrogen an ethereal solution of ethylmagnesium chloride (0.8 mL of a 2.0 M solution). The temperature was maintained at -20°C for 1 h during which time the solution turned from red purple to orange with appearance of a whitish precipitate. The resulting slurry was further stirred for 1 h at room temperature. The solvent was partially evaporated under vacuum to ca. 20 mL, and an equal volume of hexane was added to more efficiently precipitate the salts. The slurry was filtered through a pad of Celite that was further washed several times with hexane. The clear orange solution was evaporated to dryness to give either an orange oil or a powder. Recrystallization from toluene (a minimum amount)/hexane mixtures gave analytically pure orange microcrystals of **2a** in 86% yield (0.720 g, 1.25 mmol). **$\text{Tp}^*\text{Nb}(\text{Cl})(\text{Et})(\text{PhC}\equiv\text{CMe})$ (**2a**)**. ¹H NMR: major isomer δ 7.04–6.89 (m, 5H, *C*₆H₅), 5.72, 5.53, 5.42 (1H each, Tp^*CH), 3.84 (dq, $J = 12.8, 7.7$ Hz, 1H, NbHCHCH₃), 3.66 (3H, $\equiv\text{CCH}_3$), 2.77, 2.20, 2.09, 2.08, 1.87, 1.53 (3H each, Tp^*CH_3), 1.15 (dd, $J = 7.6, 6.1$ Hz, 3H, NbCH₂CH₃), 0.37 (dq, $J = 12.4, 6.2$ Hz, 1H, NbHCHCH₃); minor isomer (some resonances obscured) δ 8.20 (d, $J = 8$ Hz, 2H, *o*-*C*₆H₅), 7.44 (t, $J = 7.5$ Hz, 2H, *m*-*C*₆H₅), 7.22 (t, $J = 7.4$ Hz, 1H, *p*-*C*₆H₅), 5.71, 5.58, 5.53 (1H each, Tp^*CH), 4.02 (dq, $J = 12.6, 7.8$ Hz, 1H, NbHCHCH₃), 2.80, 2.50, 2.18, 2.08, 2.06, 2.05 (3H each, Tp^*CH_3), 1.09 (dd, $J = 7.7, 6.1$ Hz, 3H, NbCH₂CH₃). ¹³C NMR: major isomer δ 249.0 ($\equiv\text{CPh}$), 216.4 ($\equiv\text{CCH}_3$), 153.9, 153.4, 150.6, 144.8, 144.4, 144.1 (Tp^*CCH_3), 139.6 (*ipso*-*C*₆H₅), 132.4, 130.6, 129.2 (*C*₆H₅), 108.8, 108.2, 107.9 (Tp^*CH), 86.5 (dd, $w_{1/2} = 12$ Hz, $J_{\text{CH}} = 108, 129$ Hz, NbCH₂CH₃), 23.3, 18.5, 15.9, 15.6, 14.7, 13.5, 13.3, 13.1 (NbCH₂CH₃, $\equiv\text{CCH}_3$, Tp^*CH_3). Anal. Calcd for $\text{C}_{26}\text{H}_{35}\text{BClIN}_6\text{Nb}$: C, 54.7; H, 6.1; N, 14.7. Found: C, 55.1; H, 6.3; N, 14.7.

$\text{Tp}^*\text{Nb}(\text{Cl})(\text{Et})(\text{PhC}\equiv\text{CEt})$ (2b**)**. ¹H NMR: major isomer δ 7.02–6.85 (m, 5H, *C*₆H₅), 5.72, 5.54, 5.40 (1H each, Tp^*CH), 4.13 (dq (pseudosextet), $J = 15.2, 7.6$ Hz, 1H, $\equiv\text{CCH}_2\text{CH}_3$), 4.00 (dq, $J = 12.7, 7.5$ Hz, 1H, NbHCHCH₃), 3.99 (dq (pseudosextet), $J = 15.2, 7.6$ Hz, 1H, $\equiv\text{CCH}_2\text{CH}_3$), 2.75, 2.20, 2.09, 2.07, 1.84, 1.56 (3H each, Tp^*CH_3), 1.83 (t, $J = 7.6$ Hz, 3H, $\equiv\text{CCH}_2\text{CH}_3$), 1.13 (dd, $J = 7.6, 6.2$ Hz, 3H, NbCH₂CH₃), 0.37 (dq, $J = 12.7, 6.3$ Hz, 1H, NbHCHCH₃); minor isomer (some resonances obscured) δ 8.20 (d, $J = 8.2$ Hz, 2H, *o*-*C*₆H₅),

7.43 (t, $J = 7.7$ Hz, 2H, *m*-*C*₆H₅), 7.20 (t, $J = 7.4$ Hz, 1H, *p*-*C*₆H₅), 5.69, 5.58, 5.52 (1H each, Tp^*CH), 2.74, 2.17, 2.10, 2.06, 1.78, 1.55 (3H each, Tp^*CH_3), 1.08 (dd, $J = 7.6, 6.0$ Hz, 3H, NbCH₂CH₃). ¹³C NMR: major isomer δ 251.5 ($\equiv\text{CPh}$), 216.9 ($\equiv\text{CCH}_2$), 153.9, 153.2, 150.6, 144.7, 144.3, 144.1 (Tp^*CCH_3), 139.5 (*ipso*-*C*₆H₅), 130.8, 129.2 (*C*₆H₅), 108.7, 108.2, 108.0 (Tp^*CH), 86.3 (dd, $J_{\text{CH}} = 108, 130$ Hz, NbCH₂CH₃), 31.9 (t, $J_{\text{CH}} = 128$ Hz, $\equiv\text{CCH}_2\text{CH}_3$), 18.6, 15.9, 15.6, 14.8, 13.6, 13.3, 13.2, 13.1 (NbCH₂CH₃, $\equiv\text{CCH}_2\text{CH}_3$, Tp^*CH_3). Anal. Calcd for $\text{C}_{27}\text{H}_{37}\text{BClIN}_6\text{Nb}$: C, 55.5; H, 6.3; N, 14.4. Found: C, 55.8; H, 6.5; N, 14.5.

$\text{Tp}^*\text{Nb}(\text{Cl})(\text{Et})(\text{PhC}\equiv\text{C}-n\text{-Pr})$ (2c**)**. ¹H NMR: major isomer δ 7.05–6.86 (m, 5H, *C*₆H₅), 5.73, 5.55, 5.41 (1H each, Tp^*CH), 4.07 (m, 2H, $\equiv\text{CCH}_2\text{CH}_2\text{CH}_3$), 3.84 (m, 1H, NbHCHCH₃), 2.41 (sextet, $J = 7.3$ Hz, 2H, $\equiv\text{CCH}_2\text{CH}_2\text{CH}_3$), 2.77, 2.21, 2.10, 2.08, 1.88, 1.59 (3H each, Tp^*CH_3), 1.24 (t, $J = 7.3$ Hz, 3H, $\equiv\text{CCH}_2\text{CH}_2\text{CH}_3$), 1.16 (dd, $J = 7.6, 6.2$ Hz, 3H, NbCH₂CH₃), 0.38 (dq, $J = 12.6, 6.1$ Hz, 1H, NbHCHCH₃); minor isomer (some resonances obscured) δ 8.23 (d, $J = 7$ Hz, 2H, *o*-*C*₆H₅), 7.45 (t, $J = 7.5$ Hz, 2H, *m*-*C*₆H₅), 5.69, 5.60 (1H each, Tp^*CH), 2.75, 2.16, 2.06, 1.84 (3H each, Tp^*CH_3), 0.68 (t, $J = 7.4$ Hz, 3H, $\equiv\text{CCH}_2\text{CH}_2\text{CH}_3$); isomer ratio ca. 1/7. ¹³C NMR: major isomer δ 250.0 ($\equiv\text{CPh}$), 217.2 ($\equiv\text{CCH}_2$), 153.9, 153.2, 150.6, 144.7, 144.4, 144.2 (Tp^*CCH_3), 139.6 (*ipso*-*C*₆H₅), 130.8, 129.2 (*C*₆H₅), 108.7, 108.3, 107.8 (Tp^*CH), 86.9 (dd, $J_{\text{CH}} = 103, 128$ Hz, NbCH₂CH₃), 40.8 (t, $J_{\text{CH}} = 127$ Hz, $\equiv\text{CCH}_2$), 22.4 (t, $J_{\text{CH}} = 128$ Hz, $\equiv\text{CCH}_2\text{CH}_2$), 18.6, 15.9, 15.6, 14.8, 13.6, 13.3, 13.1 (NbCH₂CH₃, $\equiv\text{CCH}_2\text{CH}_2\text{CH}_3$, Tp^*CH_3). Anal. Calcd for $\text{C}_{28}\text{H}_{39}\text{BClIN}_6\text{Nb}$: C, 56.2; H, 6.63; N, 14.0. Found: C, 56.4; H, 6.7; N, 13.9.

$\text{Tp}^*\text{Nb}(\text{Cl})(\text{Et})(\text{PhC}\equiv\text{CPh})$ (2d**)**. ¹H NMR: δ 8.37 (d, $J = 7$ Hz, 2H, *o*-*C*₆H₅), 7.45 (t, $J = 7.7$ Hz, 2H, *m*-*C*₆H₅), 7.22 (t, $J = 7.5$ Hz, 1H, *p*-*C*₆H₅), 7.11–6.84 (m, 5H, *C*₆H₅), 5.72, 5.55, 5.42 (1H each, Tp^*CH), 4.25 (dq, $J = 12.6, 7.7$ Hz, 1H, NbHCHCH₃), 2.77, 2.20, 2.09, 2.09, 1.89, 1.72 (3H each, Tp^*CH_3), 1.10 (dd, $J = 7.7, 6.0$ Hz, 3H, NbCH₂CH₃), 0.47 (pseudosextet, $J = 12.5, 6.1$ Hz, 1H, NbHCHCH₃). ¹³C NMR: δ 239.3 ($\equiv\text{CPh}$), 218.9 ($\equiv\text{CPh}$), 154.3, 153.3, 150.5, 144.8, 144.5, 144.3 (Tp^*CCH_3), 141.7 (*ipso*-*C*₆H₅), 139.6 (*ipso*-*C*₆H₅), 130.0, 129.7, 129.6, 129.5, 129.3, 129.2 (*C*₆H₅), 108.8, 108.4, 108.0 (Tp^*CH), 93.7 (dd, $J_{\text{CH}} = 103, 128$ Hz, NbCH₂CH₃), 19.0, 16.0, 15.8, 14.7, 13.6, 13.3, 13.1 (NbCH₂CH₃, Tp^*CH_3). Anal. Calcd for $\text{C}_{31}\text{H}_{37}\text{BClIN}_6\text{Nb}$: C, 58.8; H, 5.9; N, 14.7. Found: C, 59.1; H, 6.0; N, 14.4.

$\text{Tp}^*\text{Nb}(\text{Cl})(\text{Et})(\text{MeC}\equiv\text{CMe})$ (2e**)**. ¹H NMR: δ 5.68, 5.62, 5.51 (1H each, Tp^*CH), 3.72 (dq, $J = 12.7, 7.7$ Hz, 1H, NbHCHCH₃), 3.30, 2.27 (s, 3H each, $\equiv\text{CCH}_3$), 2.71, 2.17, 2.09, 2.05, 2.04, 1.72 (3H each, Tp^*CH_3), 1.13 (dd, $J = 7.7, 6.3$ Hz, 3H, NbCH₂CH₃), 0.20 (pseudosextet, $J = 12.4, 6.2$ Hz, 1H, NbHCHCH₃). ¹³C NMR: δ 245.4, 224.6 ($\equiv\text{CCH}_3$), 153.1, 152.5, 149.3, 144.5, 144.3, 143.9 (Tp^*CCH_3), 108.5, 107.9, 107.8 (Tp^*CH), 84.9 (br dd, $J_{\text{CH}} = 104, 129$ Hz, NbCH₂CH₃), 22.3, 21.3 ($\equiv\text{CCH}_3$), 18.1, 15.7, 15.6, 14.3, 13.3, 13.1, 12.9 (NbCH₂CH₃, Tp^*CH_3). Anal. Calcd for $\text{C}_{21}\text{H}_{33}\text{BClIN}_6\text{Nb}$: C, 49.6; H, 6.5; N, 16.5. Found: C, 49.7; H, 6.0; N, 16.4.

$\text{Tp}^*\text{Nb}(\text{Cl})(n\text{-Pr})(\text{PhC}\equiv\text{CMe})$ (3a**)**. ¹H NMR: major isomer δ 7.04–6.89 (m, 5H, *C*₆H₅), 5.72, 5.53, 5.41 (1H each, Tp^*CH), 3.69 (app td, 1H, NbHCHCH₂CH₃), 3.68 (s, 3H, $\equiv\text{CCH}_3$), 2.76, 2.21, 2.10, 2.08, 1.85, 1.53 (3H each, Tp^*CH_3), 1.53 (m, 1H, NbCH₂CH₂CH₃), 0.86 (t, $J = 6.9$ Hz, 3H, NbCH₂CH₂CH₃), 0.71 (m, 1H, NbCH₂CH₂CH₃), 0.58 (m, 1H, NbHCHCH₂CH₃); minor isomer (some resonances obscured) δ 8.22 (d, $J = 7$ Hz, 2H, *o*-*C*₆H₅), 7.43 (t, $J = 7.6$ Hz, 2H, *m*-*C*₆H₅), 7.21 (t, $J = 7.6$ Hz, 1H, *p*-*C*₆H₅), 5.71, 5.59 (1H each, Tp^*CH), 2.80, 2.51, 2.19, 2.07, 2.05, 1.77 (3H each, Tp^*CH_3 or $\equiv\text{CCH}_3$); isomer ratio ca. 1/4. ¹³C NMR: major isomer δ 249.7 ($\equiv\text{CPh}$), 216.9 ($\equiv\text{CCH}_3$), 153.9, 153.4, 150.7, 144.7, 144.4, 144.2 (Tp^*CCH_3), 139.7 (*ipso*-*C*₆H₅), 130.6, 129.2 (*C*₆H₅), 108.7, 108.2, 107.9 (Tp^*CH), 95.9 (dd, $J_{\text{CH}} = 106, 125$ Hz, NbCH₂CH₃), 27.6 (t, $J_{\text{CH}} = 127$ Hz, NbCH₂CH₂CH₃), 23.4, 20.9, 15.9, 15.6, 14.7, 13.5, 13.3, 13.1 (NbCH₂CH₂CH₃, $\equiv\text{CCH}_3$, Tp^*CH_3). Anal. Calcd for $\text{C}_{27}\text{H}_{37}\text{BClIN}_6\text{Nb}$: C, 55.5; H, 6.3; N, 14.4. Found: C, 55.7; H, 6.7; N, 14.2.

$\text{Tp}^*\text{Nb}(\text{Cl})(n\text{-Pr})(\text{PhC}\equiv\text{CEt})$ (3b**)**. ¹H NMR: major isomer δ 7.01–6.85 (m, 5H, *C*₆H₅), 5.72, 5.54, 5.40 (1H each, Tp^*CH), 4.14 (pseudosextet, $J = 15.1, 7.5$ Hz, 1H, $\equiv\text{CCH}_2\text{CH}_3$), 4.06 (pseudosextet, $J = 15.1, 7.5$ Hz, 1H, $\equiv\text{CCH}_2\text{CH}_3$), 3.88 (app td, 1H, NbHCHCH₂CH₃), 2.77, 2.20, 2.09, 2.06, 1.86, 1.58 (3H each, Tp^*CH_3), 1.86 (t, $J = 7.5$ Hz, 3H, $\equiv\text{CCH}_2\text{CH}_3$), 1.52 (m, 1H, NbCH₂CH₂CH₃), 0.88 (t, $J = 7.0$ Hz, NbCH₂CH₂CH₃), 0.71 (m, 1H, NbCH₂CH₂CH₃), 0.60 (app

(42) Scherer, O. J.; Glabel, W. *Chem. Ztg.* **1975**, *99*, 246.

td, 1H, NbHCHCH₂CH₃); minor isomer (some resonances obscured) δ 8.25 (d, J = 8 Hz, 2H, o-C₆H₅), 7.44 (t, J = 7.7 Hz, 2H, m-C₆H₅), 5.69, 5.58, 5.51 (1H each, Tp*CH), 2.17, 2.11 (3H each, Tp*CH₃), 0.79 (t, J = 7.4 Hz, 3H, \equiv CCH₂CH₃); isomer ratio ca. 1/4. ¹³C NMR: major isomer δ 251.8 (\equiv CPh), 217.4 (\equiv CCH₃), 153.9, 153.3, 150.8, 144.7, 144.3, 144.2 (Tp*CCH₃), 139.6 (*ipso*-C₆H₅), 130.8, 129.2 (C₆H₅), 108.7, 108.3, 108.0 (Tp*CH), 95.7 (dd, J_{CH} = 108, 125 Hz, NbCH₂-CH₂CH₃), 31.9 (t, J_{CH} = 126 Hz, \equiv CCH₂CH₃), 27.6 (t, J_{CH} = 126 Hz, NbCH₂CH₂CH₃), 20.9, 16.0, 15.6, 14.8, 13.6, 13.3, 13.2, 13.1 (NbCH₂-CH₂CH₃, \equiv CCH₂CH₃, Tp*CH₃). Anal. Calcd for C₂₈H₃₉BClN₆Nb: C, 56.2; H, 6.6; N, 14.0. Found: C, 56.0; H, 6.6; N, 13.5.

Tp*Nb(Cl)(CH₂SiMe₃)(PhC=CMe) (4a). ¹H NMR: major isomer δ 7.00–6.85 (m, 5H, C₆H₅), 5.72, 5.52, 5.34 (1H each, Tp*CH), 3.75 (3H, \equiv CCH₃), 3.30 (d, J = 12.2 Hz, 1H, NbHCHSiMe₃), 2.82, 2.24, 2.16, 2.04, 1.74, 1.60 (3H each, Tp*CH₃), 0.22 (d, J = 12.3 Hz, 1H, NbHCHSiMe₃), -0.21 (9H, Si(CH₃)₃); minor isomer (some resonances obscured) δ 8.24 (d, J = 7 Hz, 2H, o-C₆H₅), 7.41 (t, J = 7.5 Hz, 2H, m-C₆H₅), 7.17 (t, J = 7 Hz, 1H, p-C₆H₅), 5.70, 5.62, 5.45 (1H each, Tp*CH), 3.66 (d, J = 11.8 Hz, 1H, NbHCHSiMe₃), 2.86, 2.49, 2.14, 2.02, 1.97, 1.88 (3H each, Tp*CH₃, \equiv CCH₃), 0.32 (d, J = 11.6 Hz, 1H, NbHCHSiMe₃), -0.40 (9H, Si(CH₃)₃); isomer ratio ca. 7/1. ¹³C NMR: major isomer δ 251.0 (\equiv CPh), 219.3 (\equiv CCH₃), 152.9, 152.6, 150.7, 144.2, 144.0, 143.8 (Tp*CCH₃), 138.9 (*ipso*-C₆H₅), 130.0, 129.1, 128.8 (C₆H₅), 108.6, 107.8, 107.6 (Tp*CH), 78.6 (dd, $w_{1/2}$ = 12 Hz, J_{CH} \approx 100, 110 Hz, NbCH₂SiMe₃), 23.7, 16.9, 15.7, 15.1, 13.0, 12.7, 12.6 (\equiv CCH₃, Tp*CH₃), 2.2 (Si(CH₃)₃). Anal. Calcd for C₂₈H₄₁BClN₆NbSi: C, 53.5; H, 6.6; N, 13.4. Found: C, 53.9; H, 6.9; N, 13.1.

Synthesis of Methyl Complexes 5b,c. MeMgCl (0.230 mL of a 3.0 M solution in THF, 0.69 mmol) was transferred in a Schlenk tube and the solution pumped to dryness. To this material cooled down to -50 °C was added a precooled toluene solution (40 mL, -80 °C) of Tp*NbCl₂(PhC=C-*n*-Pr) (**1c**) (0.420 g, 0.69 mmol). The resulting slurry was stirred at -20 °C for 1 h during which time the color turned from red purple to orange. Concentration to ca. 20 mL, addition of pentane (20 mL), and filtration through Celite gave a clear orange solution. ¹H NMR revealed the presence of Tp*Nb(Cl)(Me)(PhC=C-*n*-Pr) (**5c**) (ca. 90%), Tp*NbCl₂(PhC=C-*n*-Pr) (**1c**), and Tp*NbMe₂(PhC=C-*n*-Pr) (ca. 5% each). Concentration to ca. 3 mL and addition of pentane (15 mL) led to crystallization of orange crystals with the same composition (0.335 g, 83%). Despite careful experimental procedures, the ratios may be as low as ca. 80%, 10%, 10%.

Tp*Nb(Cl)(Me)(PhC=CEt) (5b). ¹H NMR: major isomer δ 7.0–6.80 (m, 5H, C₆H₅), 5.73, 5.45, 5.43 (1H each, Tp*CH), 4.20, 4.08 (pseudosextet each, J = 7.5, 15.0 Hz, 2H, \equiv CCH₂CH₃), 2.76, 2.21, 2.08, 2.06, 1.86, 1.82 (3H each, Tp*CH₃), 1.83 (t, J = 7.5 Hz, 3H, \equiv CCH₂CH₃), 1.62 (s, 3H, NbCH₃); minor isomer (some resonances obscured) δ 8.21 (d, J = 7 Hz, 2H, o-C₆H₅), 7.43 (t, 2H, m-C₆H₅), 5.69, 5.53, 5.48 (1H each, Tp*CH), 2.16, 2.04 (3H each, Tp*CH₃), 0.74 (t, J = 7.4 Hz, 3H, \equiv CCH₂CH₃); isomer ratio ca. 1/7. ¹³C NMR: major isomer δ 256.6 (\equiv CPh), 222.5 (\equiv CCH₂), 153.8, 153.0, 151.2, 144.8, 144.3, 144.1 (Tp*CCH₃), 139.4 (*ipso*-C₆H₅), 130.8, 129.2 (C₆H₅), 108.8, 108.3, 108.1 (Tp*CH), 61.4 (q, J_{CH} = 122 Hz, NbCH₃), 32.3 (t, J_{CH} = 128 Hz, \equiv CCH₂), 16.1, 15.6, 15.3, 13.5, 13.2, 13.1, 12.9 (\equiv CCH₂CH₃, Tp*CH₃).

Tp*Nb(Cl)(Me)(PhC=C-*n*-Pr) (5c). ¹H NMR: major isomer δ 7.05–6.86 (m, 5H, C₆H₅), 5.75, 5.48, 5.46 (1H each, Tp*CH), 4.15 (m, 2H, \equiv CCH₂CH₂CH₃), 2.42 (m, 2H, \equiv CCH₂CH₂CH₃), 2.74, 2.23, 2.11, 2.10, 1.86, 1.80 (3H each, Tp*CH₃), 1.63 (s, 3H, NbCH₃), 1.24 (t, J = 7.2 Hz, 3H, \equiv CCH₂CH₂CH₃); minor isomer (some resonances obscured) δ 8.20 (d, J = 7 Hz, 2H, o-C₆H₅), 7.43 (t, 2H, m-C₆H₅), 5.71, 5.59 (1H each, Tp*CH), 2.72, 2.07, 2.04 (3H each, Tp*CH₃), 0.67 (t, J = 7.4 Hz, 3H, \equiv CCH₂CH₂CH₃); isomer ratio ca. 1/7. ¹³C NMR: major isomer δ 255.4 (\equiv CPh), 222.8 (\equiv CCH₂), 153.7, 152.9, 151.1, 144.8, 144.3, 144.2 (Tp*CCH₃), 139.4 (*ipso*-C₆H₅), 130.8, 129.2 (C₆H₅), 108.8, 108.3, 108.1 (Tp*CH), 62.1 (q, J_{CH} = 123 Hz, NbCH₃), 41.2 (t, J_{CH} = 124 Hz, \equiv CCH₂), 22.3 (t, J_{CH} = 128 Hz, \equiv CCH₂CH₂) 16.1, 15.9, 15.6, 15.3, 13.6, 13.2, 13.1 (\equiv CCH₂CH₂CH₃, Tp*CH₃). Anal. Calcd for C₂₇H₃₇BClN₆Nb: C, 55.5; H, 6.3; N, 14.4. Found: C, 55.6; H, 6.6; N, 14.2.

Thermolysis of α -Agostic Alkyl Phenylpropyne Complexes. A similar procedure was used for the rearrangement of **2a**, **3a**, and **4a**. Tp*Nb(Cl)(Et)(PhC=CMe) (**2a**) (0.260 g, 0.46 mmol) dissolved in

toluene (20 mL) was placed in a glass vessel equipped with a Teflon stopcock. Heating overnight (80 °C, ca. 16 h) in an oil bath with stirring resulted in a darkening of the orange color. The resulting solution was filtered through Celite and analyzed by ¹H NMR. Concentration of the solution to an oil (ca. 1 mL) and addition of pentane (10 mL) gave orange crystals (0.200 g, 77%). ¹H and ¹³C NMR data revealed the same composition as that of the crude reaction mixture, i.e., Tp*Nb(Cl)(Me)(PhC=CEt) (**5b**) (ca. 80%), Tp*NbCl₂(PhC=CEt) (**1b**) (ca. 10%). Data for **5b,c** are given above, and those of **5d** resulting from the rearrangement of **4a** follow.

Tp*Nb(Cl)(Me)(PhC=CCH₂SiMe₃) (5d). ¹H NMR: δ 7.00–6.85 (m, 5H, C₆H₅), 5.74, 5.49, 5.43 (1H each, Tp*CH), 4.09 (d, J = 10.8 Hz, 1H, \equiv CCH₂SiMe₃), 3.91 (d, 1H, J = 10.8 Hz, \equiv CCH₂SiMe₃), 2.74, 2.22, 2.12, 2.05, 1.96, 1.92 (3H each, Tp*CH₃), 1.56 (3H, NbCH₃), 0.50 (9H, Si(CH₃)₃). ¹³C NMR: δ 252.4 (\equiv CPh), 224.6 (\equiv CCH₂), 153.3, 152.3, 150.4, 144.2, 143.7, 143.5 (Tp*CCH₃), 139.3 (*ipso*-C₆H₅), 129.4, 128.7, 128.6 (C₆H₅), 108.2, 107.8, 107.5 (Tp*CH), 64.6 (q, J_{CH} \approx 122 Hz, NbCH₃), 31.6 (d, J_{CH} = 122 Hz, \equiv CCH₂), 15.6, 15.5, 14.6, 13.0, 12.6, 12.4 (Tp*CH₃), 1.0 (Si(CH₃)₃).

Tp*Nb(Cl)(CPh=CEt₂)(PhC=CMe) (6). A mixture of Tp*Nb(Cl)(Et)(PhC=CEt) (**2b**) (0.480 g, 0.82 mmol) and PhC=CMe (0.200 mL, 1.6 mmol) in toluene (20 mL) was placed in a glass vessel equipped with a Teflon stopcock. Heating overnight (80 °C, ca. 16 h) in an oil bath with stirring resulted in a color change from orange to dark bright red. The resulting solution was evaporated to dryness and the residue extracted with a toluene/pentane mixture (20/80 mL). After filtration through Celite, concentration of the solution to an oil (ca. 1–2 mL), and addition of pentane (10 mL), dark red crystals of **6** were obtained, washed with a minimum amount of pentane, and then dried under vacuum (0.410 g, 0.58 mmol, 71%). No efforts were made to collect more product from the supernatant. ¹H NMR: δ 6.95–6.65 (m, 5H, \equiv CC₆H₅), 5.75, 5.66, 5.20 (1H each, Tp*CH), 3.00 (3H, \equiv CCH₃), 2.80, 2.26, 2.02, 1.93, 1.49 (3:6:3:3:3H, Tp*CH₃), 1.64 (m, 2H, CH₂CH₃), 1.18 (m, 2H, CH₂CH₃), 0.73 (t, J = 7.6 Hz, 3H, CH₂CH₃), 0.41 (t, J = 7.5 Hz, 3H, CH₂CH₃). ¹³C NMR: δ 249.7 (\equiv CPh), 224.1 (\equiv CCH₃), 204.9 (br, NbCPh), 155.7 (NbC-*ipso*-C₆H₅), 153.2, 152.8, 152.0 (Tp*CCH₃), 149.2 (\equiv C(CH₂CH₃)₂), 144.1, 143.7, 143.5 (Tp*CCH₃), 139.3 (*ipso*-C₆H₅), 129.4, 129.0, 128.6 (\equiv CC₆H₅), 129.1, 128.4, 128.2, 126.1, 123.2 (NbCC₆H₅), 108.5, 108.4, 107.5 (Tp*CH), 26.6, 23.9 (CH₂CH₃), 21.1, 17.1, 16.8, 14.5, 13.1, 12.8, 12.7, 12.5 (CH₂CH₃, \equiv CCH₃, Tp*CH₃). Anal. Calcd for C₃₆H₄₅BClN₆Nb: C, 61.7; H, 6.5; N, 12.0. Found: C, 62.2; H, 6.6; N, 11.9.

Tp*Nb(Cl)(CPh=CEt₂)[N-P(N-*i*-Pr)₂] (7). A similar procedure as that described for **6**, using **2b** (0.600 g, 1.03 mmol) and N₃P(N-*i*-Pr)₂ (0.340 g, 1.25 mmol), yielded dark bright red **7** after crystallization at -20 °C (0.620 g, 0.74 mmol, 75%). ³¹P{¹H} NMR: δ 118.7. ¹H NMR: δ 8.01 (d, J = 7.5 Hz, 1H, o-C₆H₅), 7.66 (d, J = 7.6 Hz, 1H, o-C₆H₅), 7.51 (t, J = 7.6 Hz, 1H, m-C₆H₅), 7.35 (t, J = 7.6 Hz, 1H, m-C₆H₅), 7.10 (t, J = 7.3 Hz, 1H, p-C₆H₅), 5.65, 5.58, 5.47 (1H each, Tp*CH), 3.80 (d sextet, J_{HP} = 10.2 Hz, J_{HH} = 6.8 Hz, 2H, PN[CH(CH₃)₂]₂), 3.52 (d sextet, J_{HP} = 10.2 Hz, J_{HH} = 6.8 Hz, 2H, PN[CH(CH₃)₂]₂), 3.09 (d, J_{PH} = 2.6 Hz, 3H, Tp*CH₃), 2.89, 2.63, 2.19, 2.13, 2.12 (s, 3H each, Tp*CH₃), 1.60 (pseudo q, J = 7.5 Hz, 2H, CH₂CH₃), 1.27 (d, J = 6.8 Hz, 6H, CH(CH₃)₂), 1.24 (d, J = 6.8 Hz, 6H, CH(CH₃)₂), 1.10 (d, J = 6.8 Hz, 6H, CH(CH₃)₂), 0.92 (dq, J \approx 7, 14 Hz, 2H, CH₂CH₃), 0.88 (d, J = 6.8 Hz, 6H, CH(CH₃)₂), 0.78 (t, J = 7.5 Hz, 3H, CH₂CH₃), 0.38 (t, J = 7.5 Hz, 3H, CH₂CH₃). ¹³C NMR: (NbCPh not observed) δ 154.0, 153.4, 153.3, 153.0 (NbC-*ipso*-C₆H₅, Tp*CCH₃), 151.0 (\equiv C(CH₂CH₃)₂), 145.2, 145.0, 143.3 (Tp*CCH₃), 130.9, 129.1 (d, J_{PC} = 6 Hz), 128.9, 128.1, 124.9 (NbCC₆H₅), 108.2, 108.0, 107.3 (Tp*CH), 48.1 (d, J_{PC} = 15 Hz, PN[CH(CH₃)₂]₂), 47.9 (d, J_{PC} = 14 Hz, PN[CH(CH₃)₂]₂), 26.8 (CH₂CH₃), 26.7 (d, J_{PC} = 6 Hz, PN[CH(CH₃)₂]₂), 25.3 (d, J_{PC} = 7 Hz, PN[CH(CH₃)₂]₂), 25.1 (d, J_{PC} = 6 Hz, PN[CH(CH₃)₂]₂), 25.0 (CH₂CH₃), 19.8 (d, J_{PC} = 16 Hz), 17.9, 16.7, 13.4, 13.3, 13.1, 13.0, 12.9 (CH₂CH₃, Tp*CH₃). Anal. Calcd for C₃₉H₄₅BClN₆NbP: C, 56.4; H, 7.9; N, 15.2. Found: C, 56.7; H, 8.2; N, 15.1.

Tp*Nb(Cl)(CPh=CEt₂)(O) (8). A similar procedure as that described for **6**, using **2b** (0.225 g, 0.38 mmol) and propylene oxide (0.10 mL, 1.4 mmol), yielded bright red **8** after crystallization at -20 °C (0.170 g, 0.28 mmol, 74%). ¹H NMR: δ 8.48 (d, J = 8 Hz, 1H, o-C₆H₅), 7.73 (d, J = 8 Hz, 1H, o-C₆H₅), 7.51 (t, J = 8 Hz, 1H, m- or p-C₆H₅), 7.39 (t, J = 8 Hz, 1H, m- or p-C₆H₅), 7.16 (t, obscd by solvent,

m- or p- C_6H_5), 5.66, 5.48, 5.19 (1H each, Tp*CH), 2.94, 2.82, 2.59, 2.20, 2.08, 1.92 (s, 3H each, Tp*CH₃), 1.82 (m, 2H, CH₂CH₃), 1.18 (m, 2H, CH'₂CH'₃), 0.80 (t, $J = 7.5$ Hz, 3H, CH₂CH₃), 0.39 (t, $J = 7.5$ Hz, 3H, CH'₂CH'₃). ¹³C NMR: δ 202 (weak br $w_{1/2} \approx 25$ Hz, NbCPh), 153.6 (NbC-*ipso*-C₆H₅), 153.2, 153.0, 152.7 (Tp*CCH₃), 147.1 (=C(CH₂CH₃)₂), 145.2, 144.8, 143.6 (Tp*CCH₃), 134.3, 132.9, 128.3, 128.2, 126.6 (NbCC₆H₅), 108.5, 108.4, 107.5 (Tp*CH), 27.6, 25.5 (CH₂-CH₃), 16.5, 15.9, 15.6, 12.8, 12.7, 12.5, 12.1 (CH₂CH₃, Tp*CH₃). IR (KBr, cm⁻¹) ν (NbO) 930 s. Anal. Calcd for C₂₇H₃₇-BCIN₆NbO: C, 54.0; H, 6.2; N, 14.0. Found: C, 54.5; H, 6.7; N, 13.5.

Tp*Nb(Cl)(CPh=CEt₂)(S) (9). A similar procedure as that described for **6**, using **2b** (0.210 g, 0.36 mmol) and ethylene sulfide (0.25 mL, 4.1 mmol), yielded dark red purple **9** after crystallization at -20 °C (0.155 g, 0.25 mmol, 70%). ¹H NMR: δ 8.36 (d, $J = 8$ Hz, 1H, o-C₆H₅), 7.96 (d, $J = 8$ Hz, 1H, o-C₆H₅), 7.54 (t, $J = 8$ Hz, 1H, m-C₆H₅), 7.43 (t, $J = 8$ Hz, 1H, m-C₆H₅), 7.16 (t, obscd by solvent, p-C₆H₅), 5.57, 5.53, 5.31 (1H each, Tp*CH), 3.14, 2.80, 2.71, 2.12, 2.09, 1.96 (s, 3H each, Tp*CH₃), 1.75 (m, 2H, CH₂CH₃), 0.89 (m, 2H, CH'₂CH'₃), 0.79 (t, $J = 7.5$ Hz, 3H, CH₂CH₃), 0.37 (t, $J = 7.5$ Hz, 3H, CH'₂CH'₃). ¹³C NMR: δ 212 (weak br $w_{1/2} \approx 25$ Hz, NbCPh), 154.3, 154.1, 154.0, 153.2, 152.6 (NbC-*ipso*-C₆H₅, Tp*CCH₃, =C(CH₂-CH₃)₂), 144.9, 144.8, 143.6 (Tp*CCH₃), 132.4, 131.5, 129.5, 128.3, 125.4 (NbCC₆H₅), 108.3, 107.9, 107.7 (Tp*CH), 27.7, 24.9 (CH₂CH₃), 19.1, 18.3, 16.2, 12.9, 12.7, 12.5, 12.3 (CH₂CH₃, Tp*CH₃). IR (KBr, cm⁻¹) ν (NbS) 514 s. Anal. Calcd for C₂₇H₃₇BCIN₆NbS: C, 52.6; H, 6.05; N, 13.6. Found: C, 52.7; H, 6.20; N, 13.5.

Kinetic Analyses. Thermal Rearrangement of 2a. The kinetic data at a given temperature were obtained by monitoring (¹H NMR, 250 MHz, toluene-*d*₈) the disappearance of the alkyne methyl and the deshielded methylene signals around δ 3.8. The disappearance was quantified by integration against the whole Tp*CH resonances between *ca.* δ 6.1–5.1; *ca.* 15 mg of **2a** was dissolved under dinitrogen in toluene-*d*₈ (0.4 mL, [**2a**] $\approx 4 \times 10^{-2}$ M) in a 5 mm NMR tube which was sealed with a septum and parafilm. The tube was introduced in the preheated probe of the NMR spectrometer. After 15 min of thermal equilibration, an automatic acquisition program was used to collect the spectra at given intervals. Given the rate of the reactions, 32 scan spectra with an acquisition time of 3.064 s and a repetition delay of 2.0 s were recorded every 30 min ($T = 343, 348, 353$ K) or 40 min ($T = 338$ K). The reaction was monitored for *ca.* 3 half-lives. The results of the first-order treatment can be found in Table 4 and Figure 3, and the corresponding Eyring plot is shown in Figure 4. A strictly identical procedure was used for the thermolysis of **3a** and **4a** at 343 K.

Thermal Rearrangement of 2b: Trapping with Phenylpropyne. The kinetic data at 343 K were obtained as for the thermal rearrangement of **2a** by monitoring the disappearance of the methylene signals in the region *ca.* δ 3.8–4.6; *ca.* 15 mg of **2b** was dissolved under dinitrogen in toluene-*d*₈ (0.4 mL, [**2b**] $\approx 4 \times 10^{-2}$ M) in a 5 mm NMR tube, and a given amount of phenylpropyne was added (between *ca.* 6 to 12 equiv). The tube was sealed with a septum and parafilm. The same acquisition sequence as for the rearrangement of **2a** was used. The results of the pseudo-first-order treatment can be found in Table 5.

X-ray Crystallographic Analyses. Crystals of **4a** were obtained from an ethereal solution, and those of **9** from a toluene/hexane solution. A four-circle ENRAF-NONIUS CAD 4 diffractometer using Mo K α radiation and a graphite monochromator was used to collect the diffraction data for C₃₂H₅₁BCIN₆NbOSi (**4a**·Et₂O) (173 K) and C₃₉H₆₅-

BCIN₆NbP (**7**) (293 K). Unit cell dimensions with standard deviations were obtained from a least-squares refinement of the setting angles of 25 well-centered reflections. Corrections were made for Lorentz and polarization effects. Computations were performed by using CRYSTALS⁴³ adapted on a PC. The atomic scattering factors were taken from the literature.⁴⁴ Full matrix least-squares refinement was carried out by minimizing the function $\sum w(|F_o| - |F_c|)^2$, where F_o and F_c are the observed and calculated structure factors, respectively. The weighting scheme used in the last refinement cycles was $w = w'[1 - (\Delta F/6\sigma(F_o))^2]$ where $w' = 1/\sum(r = 1,3)ArTr(x)$, with a variable number of coefficients Ar for the Chebyshev polynomial Tr(x) with $x = F_c/F_{c(max)}$.⁴⁵ Details are summarized in Table 1.

For **4a**·Et₂O, the structure was solved by direct methods (SIR92)⁴⁶ and subsequent Fourier syntheses. Absorption corrections were made by using psi scans. One molecule of diethyl ether was located after the first cycle. All non-hydrogen atoms were anisotropically refined. Several hydrogen atoms were located by a Fourier difference, but only those bound to C(1) were considered for a refinement of their positional and isotropic thermal parameters. All other hydrogen atoms were set in idealized positions with thermal parameters 20% higher than those of the atom to which they were attached.

For **7**, the structure was solved by direct methods (SHELXS 86)⁴⁷ and subsequent differences Fourier maps. No absorption corrections were made. All non-hydrogen atoms were anisotropically refined except the carbon atoms of the phenyl and isopropyl groups which were refined isotropically. Hydrogen atoms were located by Fourier syntheses, but their coordinates were recalculated after each cycle. They were assign isotropic thermal parameters 20% higher than those of the atom to which they were attached.

Acknowledgment. The authors wish to thank the following people: G. Commenges and F. Lacassin (NMR Facility at the LCC) for operating the Bruker AMX 400 machine, J. Jaud (CEMES-CNRS, Toulouse) for the low-temperature acquisition of the X-ray data for **4a**·Et₂O, Drs. G. Bouhadir, R. Réau, and G. Bertrand (LCC) for a generous gift of N₃P(N-*i*-Pr₂).

Supporting Information Available: Expanded regions of the ¹H-gated ¹³C NMR spectra of **3a** and **2c** showing the NbCH₂R region, ¹H NMR spectrum of **4a** and expanded regions showing the ¹³C satellites of the main NbCH₂SiMe₃ resonances, and positional and thermal parameters and interatomic bond distances and angles for **4a**·Et₂O and **7** (17 pages). See any current masthead page for ordering and Internet access instructions.

JA963697Q

(43) (a) Watkin, D. J.; Carruthers, R. J.; Betteridge, P. W. *Crystals Users Guide*; Chemical Crystallography Laboratory: Oxford, 1985. (b) Watkin, D. J.; Prout, C. K.; Carruthers, R. J.; Betteridge, P. W. *Crystals Issue 10*; Chemical Crystallography Laboratory: Oxford, 1996.

(44) *International Tables for X-Ray Crystallography*; Kynoch Press: Birmingham, England, 1974; Vol IV.

(45) Prince, E. *Mathematical Techniques in Crystallography*; Springer-Verlag: Berlin, 1982.

(46) Altomare, A.; Cascarano, G.; Giacovazzo, G.; Gualardi, A.; Burla, M. C.; Polidori, G.; Camalli, C. *J. Appl. Chem.* **1994**, *27*, 435.

(47) Sheldrick, G. M. *SHELXS-86 Program for Crystal Structure Solution*; University of Göttingen: Göttingen, Germany, 1986.